CHAOS, BIFURCATIONS, AND THEIR CONTROL

NONLINEAR DYNAMICS

Unlike linear systems, many nonlinear dynamical systems do not show orderly, regular, and long-term predictable responses to simple inputs. Instead, they display complex, random-like, seemingly irregular, yet well-defined output behaviors. This dynamical phenomenon is known as *chaos*.

The term chaos, originating from the Greek word $\chi\alpha o\zeta$, was designated as "the primeval emptiness of the universe before things came into being of the abyss of Tartarus, the underworld. . . . In the later cosmologies Chaos generally designated the original state of things, however conceived. The modern meaning of the word is derived from Ovid, who saw Chaos as the original disordered and formless mass, from which the maker of the Cosmos produced the ordered universe" (1). There also is an interpretation of chaos in ancient Chinese literature, which refers to the spirit existing in the center of the universe (2). In modern scientific terminology, chaos has a fairly precise but rather complicated definition by means of the dynamics of a generally nonlinear system. For example, in theoretical physics, "chaos is a type of moderated randomness that, unlike true randomness, contains complex patterns that are mostly unknown" (3).

Bifurcation, as a twin of chaos, is another prominent phenomenon of nonlinear dynamical systems: Quantitative change of system parameters leads to qualitative change of system properties such as the number and the stability of system response equilibria. Typical bifurcations include transcritical, saddle-node, pitchfork, hysteresis, and Hopf bifurcations. In particular, period-doubling bifurcation is a route to chaos. To introduce the concepts of chaos and bifurcations as well as their control (4,5), some preliminaries on nonlinear dynamical systems are in order.

Nonlinear Dynamical Systems

A *nonlinear system* refers to a set of nonlinear equations, which can be algebraic, difference, differential, integral, functional, and abstract operator equations, or a certain combination of these. A nonlinear system is used to describe a physical device or process that otherwise cannot be well defined by a set of linear equations of any kind. The term *dynamical system* is used as a synonym of mathematical or physical system, in which the output behavior evolves with time and/or other varying system parameters (6).

In general, a continuous-time dynamical system can be described by either a differential equation

$$\dot{\boldsymbol{x}} = \boldsymbol{f}(\boldsymbol{x}, t; \boldsymbol{p}), \quad t \in [t_0, \infty) \tag{1}$$

or a map

$$F : \boldsymbol{x} \to \boldsymbol{g}(\boldsymbol{x}, t; \boldsymbol{p}), \quad t \in [t_0, \infty) \tag{2}$$

where $\boldsymbol{x} = \boldsymbol{x}(t)$ is the *state* of the system, $\boldsymbol{p}$ is a vector of variable system parameters, and $\boldsymbol{f}$ and $\boldsymbol{g}$ are continuous (or differentiable) nonlinear functions of comparable dimensions, which have explicit formulation for a specified physical system.

For the discrete-time setting, a nonlinear dynamical system is described by either a difference equation

$$\boldsymbol{x}_{k+1} = \boldsymbol{f}(\boldsymbol{x}_k, k; \boldsymbol{p}), \quad k = 0, 1, \ldots \tag{3}$$

or a map

$$F : \boldsymbol{x}_k \to \boldsymbol{g}(\boldsymbol{x}_k, k; \boldsymbol{p}), \quad k = 0, 1, \ldots \tag{4}$$

where notation is similarly defined. Repeatedly iterating the discrete map F backward yields

$$\boldsymbol{x}_k = F(\boldsymbol{x}_{k-1}) = F(F(\boldsymbol{x}_{k-2})) = \cdots = F^k(\boldsymbol{x}_0)$$

where the map can also be replaced by a function, $\boldsymbol{f}$, if the system is given via a difference equation, leading to

$$\boldsymbol{x}_k = \underbrace{\boldsymbol{f} \circ \cdots \circ \boldsymbol{f}}_{k \text{ times}}(\boldsymbol{x}_0) = \boldsymbol{f}^k(\boldsymbol{x}_0)$$

where "$\circ$" denotes composition operation of functions or mappings.

The dynamical system of Eq. (1) is said to be *nonautonomous* when the time variable, t, appears separately in the system function $\boldsymbol{f}$ (e.g., a system with an external time-varying force input); otherwise, it is said to be *autonomous* and is expressed as

$$\dot{\boldsymbol{x}} = \boldsymbol{f}(\boldsymbol{x}; \boldsymbol{p}), \quad t \in [t_0, \infty) \tag{5}$$

Classification of Equilibria

For illustration, consider a general two-dimensional autonomous system

$$\begin{cases} \dot{x} = f(x, y) \\ \dot{y} = g(x, y) \end{cases} \tag{6}$$

with given initial conditions (x_0, y_0), where f and g are two smooth nonlinear functions that together describe the *vector field* of the system.

The path traveled by a solution of Eq. (6), starting from the initial state (x_0, y_0), is a *solution trajectory,* or *orbit,* of the system and is sometimes denoted by $\phi_t(x_0, y_0)$. For autonomous systems, two different orbits will never cross each other (i.e., never intersect) in the *x-y* plane. This *x-y* coordinate plane is called the (*generalized*) *phase plane* (*phase space* in the higher-dimensional case). The orbit family of a general autonomous system, corresponding to all possible initial conditions, is called *solution flow* in the phase space.

Equilibria, or *fixed points,* of Eq. (6), if they exist, are the solutions of two homogeneous equations:

$$f(x, y) = 0 \quad \text{and} \quad g(x, y) = 0$$

An equilibrium is denoted by $(\bar{x}, \bar{y})$. It is *stable* if all the nearby orbits of the system, starting from any initial conditions, approach it; it is *unstable* if the nearby orbits are moving away from it. Equilibria can be classified, according to their stabilities, as stable or unstable *node* or *focus, saddle*

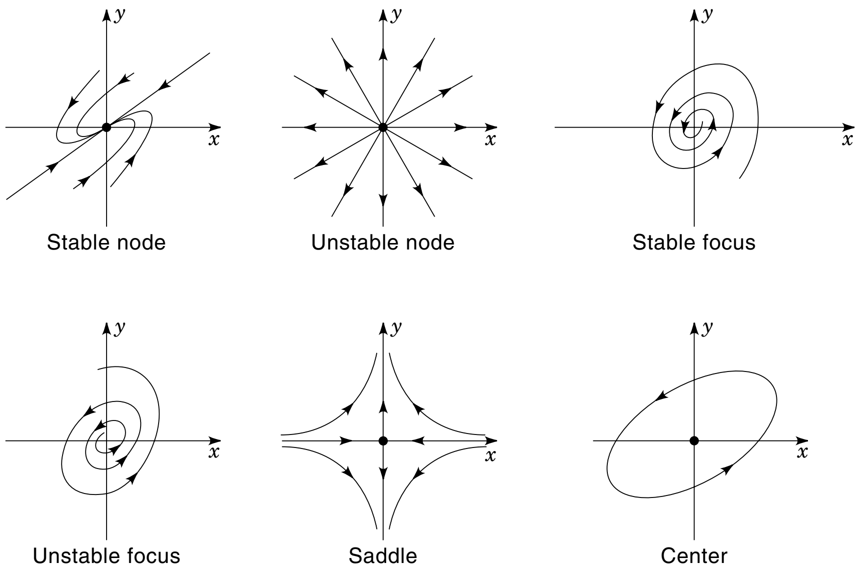

Figure 1. Classification of two-dimensional equilibria: Stabilities are determined by Jacobian eigenvalues.

point and *center,* as summarized in Fig. 1. The type of equilibria is determined by the eigenvalues, $\lambda_{1,2}$, of the system Jacobian

$$J := \begin{bmatrix} f_x & f_y \\ g_x & g_y \end{bmatrix}$$

with $f_x := \partial f/\partial x$, $f_y := \partial f/\partial y$, and so on, all evaluated at $(\bar{x}, \bar{y})$. If the two Jacobian eigenvalues have real parts $\mathscr{R}\{\lambda_{1,2}\} \neq 0$, the equilibrium $(\bar{x}, \bar{y})$ at which the linerization was taken, is said to be *hyperbolic.*

Theorem 1 (Grobman-Hartman) If $(\bar{x}, \bar{y})$ is a hyperbolic equilibrium of the nonlinear dynamical system of Eq. (6), then the dynamical behavior of the nonlinear system is qualitatively the same as (i.e., topologically equivalent to) that of its linearized system,

$$\begin{bmatrix} \dot{x} \\ \dot{y} \end{bmatrix} = J \begin{bmatrix} x \\ y \end{bmatrix}$$

in a neighborhood of the equilibrium $(\bar{x}, \bar{y})$.

This theorem guarantees that for the hyperbolic case, one can study the linearized system instead of the original nonlinear system, with regard to the *local* dynamical behavior of the system within a (small) neighborhood of the equilibrium $(\bar{x}, \bar{y})$. In other words, there exist some *homeomorphic maps* that transform the orbits of the nonlinear system into orbits of its linearized system in a (small) neighborhood of the equilibrium. Here, a homeomorphic map (or a *homeomorphism*) is a continuous map whose inverse exists and is also continuous. However, in the nonhyperbolic case the situation is much more complicated, where such local dynamical equivalence does not hold in general.

Periodic Orbits and Limit Cycles

A solution orbit, $\boldsymbol{x}(t)$, of the nonlinear dynamical system of Eq. (1) is a periodic solution if it satisfies $\boldsymbol{x}(t + t_p) = \boldsymbol{x}(t)$ for some constant $t_p > 0$. The minimum value of such t_p is called the (*fundamental*) *period* of the periodic solution, while the solution is said to be t_p-*periodic.*

A *limit cycle* of a dynamical system is a periodic solution of the system that corresponds to a closed orbit in the phase space and possesses certain attracting (or repelling) properties. Figure 2 shows some typical limit cycles for the two-dimensional case: (a) an inner limit cycle, (b) an outer limit cycle, (c) a stable limit cycle, (d) an unstable limit cycle, and (e) and (f) saddle limit cycles.

Limit Sets and Attractors

The most basic problem in studying the general nonlinear dynamical system of Eq. (1) is to understand and/or to solve for the system solutions. The asymptotic behavior of a system solution, as $t \to \infty$, is called the *steady state* of the solution, while the solution trajectory between its initial state and the steady state is the *transient state.*

For a given dynamical system, a point $\boldsymbol{x}_\omega$ in the state space is an *ω-limit point* of the system state orbit $\boldsymbol{x}(t)$ if, for every open neighborhood U of $\boldsymbol{x}_\omega$, the trajectory of $\boldsymbol{x}(t)$ will enter U at a (large enough) value of t. Consequently, $\boldsymbol{x}(t)$ will repeatedly enter U infinitely many times, as $t \to \infty$. The set of all such ω-limit points of $\boldsymbol{x}(t)$ is called the *ω-limit set* of $\boldsymbol{x}(t)$ and is denoted Ω_x. An ω-limit set of $\boldsymbol{x}(t)$ is *attracting* if there exists an open neighborhood V of Ω_x such that whenever a system orbit enters V then it will approach Ω_x as $t \to \infty$. The *basin of attraction* of an attracting set is the union of all such open neighborhoods. An ω-limit set is *repelling* if the nearby system orbits always move away from it. An *attractor* is an ω-limit set having the property that all orbits nearby have it as their ω-limit sets.

For a given map, F, and a given initial state, $\boldsymbol{x}_0$, an ω-limit set is obtained from the orbit $\{F^k(\boldsymbol{x}_0)\}$ as $k \to \infty$. This ω-limit set, Ω_x, is an invariant set of the map, in the sense that $F(\Omega_x) \subseteq \Omega_x$. Thus, ω-limit sets include equilibria and periodic orbits.

Poincaré Maps

Assume that the general n-dimensional nonlinear autonomous system of Eq. (5) has a t_p-periodic limit cycle, Γ, and let

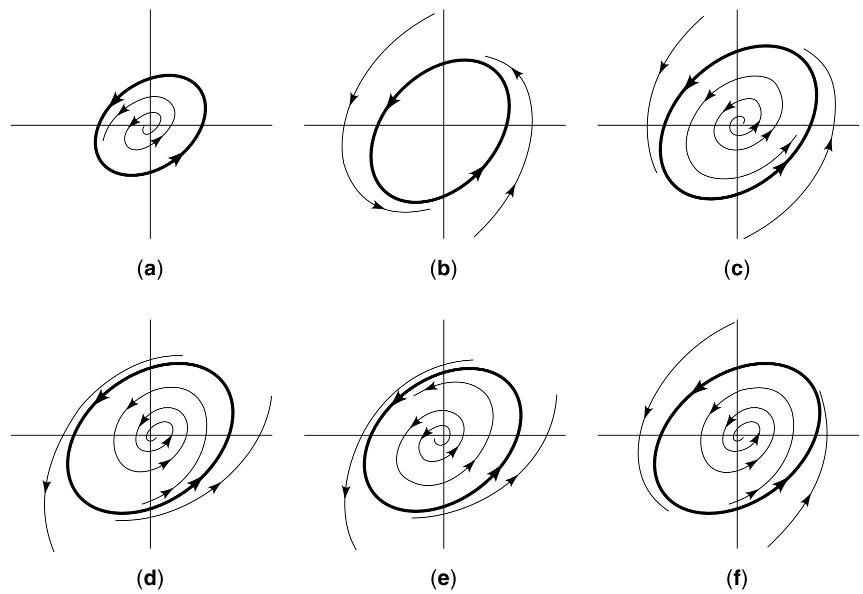

Figure 2. Periodic orbits and limit cycles.

x^* be a point on the limit cycle and Σ be an $(n-1)$-dimensional hyperplane transversal to Γ at x^*, as shown in Fig. 3. Here, the *transversality* of Σ to Γ at x^* means that Σ and the tangent line of Γ at x^* together span the entire n-dimensional space (hence, this tangent line of Γ cannot be tangent to Σ at x^*). Since Γ is t_p-periodic, the orbit starting from x^* will return to x^* in time t_p. Any orbit starting from a point, x, in a small neighborhood U of x^* on Σ will return and hit Γ at a point, denoted $P(x)$, in the vicinity V of x^*. Therefore, a map $P: U \rightarrow V$ can be uniquely defined by Σ, along with the solution flow of the autonomous system. This map is called the *Poincaré map* associated with the system and the cross section Σ. For different choices of the cross section Σ, Poincaré maps are similarly defined. Note that a Poincaré map is only locally defined and is a *diffeomorphism*—namely, a differentiable map that has an inverse and the inverse is also differentiable. If a cross section is suitably chosen, the orbit will repeatedly return and pass through the section. The Poincaré map together with the first return orbit is particularly important, which is called the *first return Poincaré map.* Poincaré maps can also be defined for nonautonomous systems in a similar way, where, however, each return map depends on the initial time in a nonuniform fashion.

Homoclinic and Heteroclinic Orbits

Let x^* be a hyperbolic equilibrium of a diffeomorphism $P: R^n \rightarrow R^n$, which can be of either unstable, center, or saddle type; $\varphi_t(x)$ be a solution orbit passing through x^*; and $\Omega_x{}^*$ be the ω-limit set of $\varphi_t(x)$. The *stable manifold* of $\Omega_x{}^*$, denoted M_s, is the set of such points x^* that satisfy $\varphi_t(x^*) \rightarrow \Omega_x{}^*$ as $t \rightarrow \infty$; the *unstable manifold* of $\Omega_x{}^*$, M_u, is the set of points x^* satisfying $\varphi_t(x^*) \rightarrow \Omega_x{}^*$ as $t \rightarrow -\infty$.

Suppose that $\Sigma_s(x^*)$ and $\Sigma_u(x^*)$ are cross sections of the stable and unstable manifolds of $\varphi_t(x)$, respectively, which intersect at x^*. This intersection always includes one constant orbit, $\varphi_t(x) = x^*$. A nonconstant orbit lying in the intersection is called a *homoclinic orbit* and is illustrated in Fig. 4(a). For two equilibria, $\bar{x}_1 \neq \bar{x}_2$, of either unstable, center, or saddle type, an orbit lying in $\Sigma_s(\bar{x}_1) \cap \Sigma_u(\bar{x}_2)$, or in $\Sigma_u(\bar{x}_1) \cap \Sigma_s(\bar{x}_2)$, is called a *heteroclinic orbit.* A heteroclinic orbit is dipicted in Fig. 4(b), which approaches one equilibrium as $t \rightarrow \infty$ but converges to another equilibrium as $t \rightarrow -\infty$.

It is known that if a stable and an unstable manifold intersect at a point, $x_0 \neq x^*$, then they will do so at infinitely many points, denoted $\{x_k\}_{k=-\infty}^{\infty}$ counted in both forward and backward directions, which contains x_0. This sequence, $\{x_k\}$, is a *homo-*

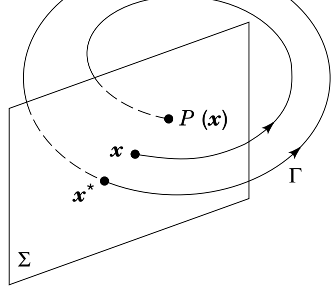

Figure 3. Schematic illustration of the Poincaré map and cross section.

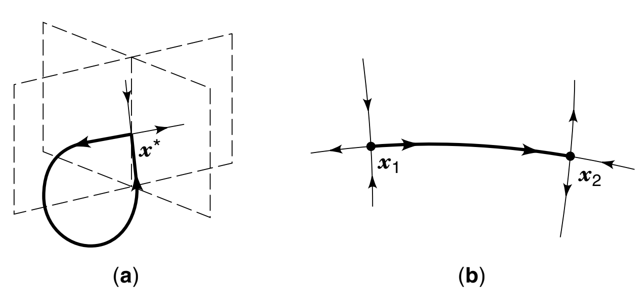

Figure 4. Schematic illustration of homoclinic and heteroclinic orbits.

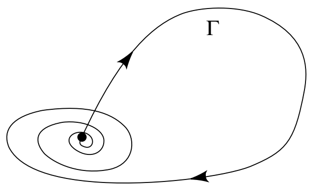

Figure 5. Illustration of a Šil'inkov-type homoclinic orbit.

clinic orbit in which each x_k is called a *homoclinic point.* This special structure is called a *homoclinic structure,* in which the two manifolds usually do not intersect transversally. Here, two manifolds are said to *intersect transversally* if their tangent planes together span the entire space (hence, these two tangent planes cannot coincide at the intersection). This structure is unstable in the sense that the connection can be destroyed by very small perturbations. If they intersect transversally, however, a transversal homoclinic point will imply infinitely many other homoclinic points. This eventually leads to a picture of stretching and folding of the two manifolds. Such complex stretching and folding of manifolds are key to chaos, which generally implies the existence of a complicated Smale horseshoe map and is supported by the following mathematical theory (7).

Theorem 2 (Smale-Birkhoff) Let $P : R^n \rightarrow R^n$ be a diffeomorphism with a hyperbolic equilibrium x^*. If the cross sections of the stable and unstable manifolds, $\Sigma_s(x^*)$ and $\Sigma_u(x^*)$, intersect transversally at a point other than x^*, then P has a horseshoe map embedded within it.

For three-dimensional autonomous systems, the case of an equilibrium with one real eigenvalue, λ, and two complex conjugate eigenvalues, $\alpha \pm j\beta$, is especially interesting. For example, the case with $\lambda > 0$ and $\alpha < 0$ gives a *Šil'nikov type* of homoclinic orbit, which is illustrated in Fig. 5.

Theorem 3 (Šil'nikov) Let φ_t be the solution flow of a three-dimensional autonomous system that has a Šil'nikov-type homoclinic orbit Γ. If $|\alpha| < |\lambda|$, then φ_t can be extremely slightly perturbed to $\tilde{\varphi}_t$, such that $\tilde{\varphi}_t$ has a homoclinic orbit $\tilde{\Gamma}$, near Γ, of the same type, and the Poincaré map defined by a cross section, transversal to $\tilde{\Gamma}$, has a countable set of Smale horseshoes.

Stabilities of Systems and Orbits

Stability theory plays a central role in both dynamical systems and automatic control. Conceptually, there are different types of stabilities, among which Lyapunov stabilities and the orbital stability are essential for chaos and bifurcations control.

Lyapunov Stabilities. In the following discussion of Lyapunov stabilities for the general nonautonomous system of Eq. (1), the parameters are dropped since they do not affect the concept and consequence. Thus, consider the general nonautonomous nonlinear system

$$\dot{x} = f(x, t), \quad x(t_0) = x_0 \tag{7}$$

and, by changing variables if necessary, assume the origin, $\bar{x} = 0$, is an equilibrium of the system satisfying $f(0, t) = 0$. Lyapunov stability theory concerns various stabilities of the zero equilibrium of Eq. (7).

Stability in the Sense of Lyapunov. The equilibrium $\bar{x} = 0$ of Eq. (7) is said to be *stable in the sense of Lyapunov* if for any $\epsilon > 0$ and any initial time $t_0 \geq 0$, there exists a constant, $\delta = \delta(\epsilon, t_0) > 0$, such that

$$\|x(t_0)\| < \delta \quad \Rightarrow \quad \|x(t)\| < \epsilon, \quad \forall t \geq t_0 \tag{8}$$

Here and throughout, $\|\cdot\|$ denotes the standard Euclidean norm of a vector.

It should be emphasized that the constant δ in the preceeding equation generally depends on both ϵ and t_0. It is particularly important to point out that, unlike autonomous systems, one cannot simply assume the initial time $t_0 = 0$ for a nonautonomous system in a general situation. The stability is said to be *uniform,* with respect to the initial time, if this constant, $\delta = \delta(\epsilon)$, is indeed independent of t_0 over the entire time interval of interest.

Asymptotic Stability. In both theoretical studies and applications, the concept of asymptotic stability is of most importance.

The equilibrium $\bar{x} = 0$ of Eq. (7) is said to be *asymptotically stable* if there exists a constant, $\delta = \delta(t_0) > 0$, such that

$$\|x(t_0)\| < \delta \quad \Rightarrow \quad \|x(t)\| \rightarrow 0 \quad \text{as } t \rightarrow \infty \tag{9}$$

This asymptotical stability is said to be *uniform* if the existing constant δ is independent of t_0, and is said to be *global* if the convergence ($\|x\| \rightarrow 0$) is independent of the starting point $x(t_0)$ over the entire domain on which the system is defined (e.g., when $\delta = \infty$).

Orbital Stability. The orbital stability differs from the Lyapunov stabilities in that it concerns the structural stability of a system orbit under perturbation.

Let $\varphi_t(x_0)$ be a t_p-periodic solution of the autonomous system

$$\dot{x}(t) = f(x), \quad x(t_0) = x_0 \tag{10}$$

and let Γ be the closed orbit of $\varphi_t(x_0)$ in the phase space—namely,

$$\Gamma = \{y | y = \varphi_t(x_0), \quad 0 \leq t < t_p\}$$

The solution trajectory $\varphi_t(x_0)$ is said to be *orbitally stable* if for any $\epsilon > 0$ there exits a $\delta = \delta(\epsilon) > 0$, such that for any $\tilde{x}_0$ satisfying

$$d(\tilde{x}_0, \Gamma) := \inf_{y \in \Gamma} \|\tilde{x}_0 - y\| < \delta$$

the solution $\varphi_t(\tilde{x}_0)$ of the autonomous system satisfies

$$d(\varphi_t(\tilde{x}_0), \Gamma) < \epsilon, \quad \forall t \geq t_0$$

Lyapunov Stability Theorems. Two cornerstones in the Lyapunov stability theory for dynamical systems are the Lyapunov first (or indirect) method and the Lyapunov second (or direct) method.

The Lyapunov first method, known also as the *Jacobian* or local *linearization method,* is applicable only to autonomous systems. This method is based on the fact that the stability of an autonomous system, in a neighborhood of an equilibrium, is essentially the same as its linearized model operating at the same point, and under certain conditions local system stability behavior is qualitatively the same as that of its linearized model (in some sense, similar to the Grobman-Hartman theorem). The Lyapunov first method provides a theoretical justification for applying linear analysis and linear feedback controllers to nonlinear autonomous systems in the study of asymptotic stability and stabilization. The Lyapunov second method, on the other hand, which originated from the concept of energy decay (i.e., dissipation) associated with a stable mechanical or electrical system, is applicable to both autonomous and nonautonomous systems. Hence, the second method is more powerful, also more useful, for rigorous stability analysis of various complex dynamical systems.

For the general autonomous system of Eq. (10), under the assumption that $\boldsymbol{f} : \mathscr{D} \to R^n$ is continuously differentiable in a neighborhood, $\mathscr{D}$, of the origin in R^n, the following theorem of stability for the Lyapunov first method is convenient to use.

Theorem 4 (Lyapunov First Method) (for continuous-time autonomous systems)

In Eq. (10), let

$$\boldsymbol{J}_0 = \left.\frac{\partial \boldsymbol{f}}{\partial \boldsymbol{x}}\right|_{\boldsymbol{x}=\overline{\boldsymbol{x}}=0}$$

be the Jacobian of the system at the equilibrium $\overline{\boldsymbol{x}} = 0$. Then (1) $\overline{\boldsymbol{x}}^* = 0$ is asymptotically stable if all the eigenvalues of $\boldsymbol{J}_0$ have negative real parts; and (2) $\boldsymbol{x} = 0$ is unstable if one of the eigenvalues of $\boldsymbol{J}_0$ has a positive real part.

Note that the region of asymptotic stability given in this theorem is local. It is important to emphasize that this theorem cannot be applied to nonautonomous systems in general, not even locally. For the general nonautonomous system of Eq. (7), the following criterion can be used. Let

$$\begin{aligned}\mathscr{K} = \{&g(t) : g(t_0) = 0,\\ &g(t) \text{ is continuous and nondecreasing on } [t_0, \infty)\}\end{aligned}$$

Theorem 5 (Lyapunov Second Method) (for continuous-time nonautonomous systems)

Let $\overline{\boldsymbol{x}} = 0$ be an equilibrium of the nonautonomous system of Eq. (7). The zero equilibrium of the system is globally (over the domain $\mathscr{D} \subseteq R^n$ containing the origin), uniformly (with respect to the initial time), and asymptotically stable if there exist a scalar-valued function $V(\boldsymbol{x}, t)$ defined on $\mathscr{D} \times [t_0, \infty)$ and three functions $\alpha(\cdot)$, $\beta(\cdot)$, $\gamma(\cdot) \in \mathscr{K}$, such that (1) $V(0, t_0) = 0$; (2) $V(\boldsymbol{x}, t) > 0$ for all $\boldsymbol{x} \neq 0$ in $\mathscr{D}$ and all $t \geq t_0$; (3) $\alpha(\|\boldsymbol{x}\|) \leq V(\boldsymbol{x}, t) \leq \beta(\|\boldsymbol{x}\|)$ for all $t \geq t_0$; and (4) $\dot{V}(\boldsymbol{x}, t) \leq -\gamma(\|\boldsymbol{x}\|)$ for all $t \geq t_0$.

In this theorem, the uniform stability is usually necessary since the solution of a nonautonomous system may depend sensitively on the initial time. As a special case for autonomous systems, the preceding theorem reduces to the following.

Theorem 6 (Lyapunov Second Method) (for continuous-time autonomous systems)

Let $\overline{\boldsymbol{x}} = 0$ be an equilibrium for the autonomous system of Eq. (10). This zero equilibrium is globally (over the domain $\mathscr{D} \subseteq R^n$ containing the origin) and asymptotically stable if there exists a scalar-valued function $V(\boldsymbol{x})$ defined on $\mathscr{D}$ such that (1) $V(0) = 0$; (2) $V(\boldsymbol{x}) > 0$ for all $\boldsymbol{x} \neq 0$ in $\mathscr{D}$; and (3) $\dot{V}(\boldsymbol{x}) < 0$ for all $\boldsymbol{x} \neq 0$ in $\mathscr{D}$.

In the preceding two theorems, the function V is called a *Lyapunov function,* which is generally not unique for a given system. Similar stability theorems can be established for discrete-time systems (by properly replacing derivatives with differences).

To this end, it is important to remark that the Lyapunov theorems only offer *sufficient* conditions for determining the asymptotic stability. Yet the power of the Lyapunov second method lies in its generality: It works for all kinds of dynamical systems (linear and nonlinear, continuous-time and discrete-time, autonomous and nonautonomous, time-delayed, functional, etc.), and it does not require any knowledge of the solution formula of the underlying system. In a particular application, the key is to construct a working Lyapunov function for the system, which can be technically difficult if the system is higher-dimensional and structurally complicated.

CHAOS

Nonlinear systems have various complex behaviors that would never have been anticipated in (finite-dimensional) linear systems. Chaos is a typical behavior of this kind. In the development of chaos theory, the first evidence of physical chaos was Edward Lorenz's discovery in 1963. The first underlying mechanism within chaos was observed by Mitchell Feigenbaum, who in 1976 found that "when an ordered system begins to break down into chaos, a consistent pattern of rate doubling occurs" (3).

What Is Chaos?

There is no unified, universally accepted, rigorous definition of chaos in the current scientific literature. The term chaos was first formally introduced into mathematics by Li and Yorke (8). Since then, there have been several different but closely related proposals for definitions of chaos, among which Devaney's definition is perhaps the most popular one (9). It states that a map $F : S \to S$, where S is a set, is said to be *chaotic* if

1. F is transitive on S: For any pair of nonempty open sets U and V in S, there is an integer $k > 0$ such that $F^k(U) \cap V$ is nonempty.
2. F has sensitive dependence on initial conditions: There is a real number $\delta > 0$, depending only on F and S, such that in every nonempty open subset of S there is a pair of points whose eventual iterates under F are separated by a distance of at least δ.
3. The periodic points of F are dense in S.

Another definition requires the set S be compact but drops condition 3. There is a belief that only the transitive property is essential in this definition. Although a precise and rigorous mathematical definition of chaos does not seem to be available anytime soon, some fundamental features of chaos are well received and can be used to signify or identify chaos in most cases.

Features of Chaos

A hallmark of chaos is its fundamental property of extreme sensitivity to initial conditions. Other features of chaos include the embedding of a dense set of unstable periodic orbits in its strange attractor, positive leading (maximal) Lyapunov exponent, finite Kolmogorov-Sinai entropy or positive topological entropy, continuous power spectrum, positive algorithmic complexity, ergodicity and mixing (Arnold's cat map), Smale horseshoe map, a statistical-oriented definition of Šhil'nikov, as well as some unusual limiting properties (4).

Extreme Sensitivity to Initial Conditions. The first hallmark of chaos is its extreme sensitivity to initial conditions, associated with its bounded (or compact) region of orbital patterns. It implies that two sets of slightly different initial conditions can lead to two dramatically different asymptotic states of the system orbit after some time. This is the so-called butterfly effect and says that a single flap of a butterfly's wings in China today *may* alter the initial conditions of the global weather dynamical system, thereby leading to a significantly different weather pattern in Argentina at a future time. In other words, for a dynamical system to be chaotic it must have a (large) set of such "unstable" initial conditions that cause orbital divergence within a bounded region.

Positive Leading Lyapunov Exponents. Most sensitive dependence on initial conditions of a chaotic system possesses an exponential growth rate. This exponential growth is related to the existence of at least one positive Lyapunov exponent, usually the leading (largest) one. Among all main characteristics of chaos, the positive leading Lyapunov exponent is perhaps the most convenient one to verify in engineering applications.

To introduce this concept, consider an n-dimensional, discrete-time dynamical system described by $\boldsymbol{x}_{k+1} = \boldsymbol{f}(\boldsymbol{x}_k)$ via a smooth map $\boldsymbol{f}$. The ith Lyapunov exponent of the orbit $\{\boldsymbol{x}_k\}_{k=0}^{\infty}$, generated by the iterations of the map starting from any given initial state $\boldsymbol{x}_0$, is defined to be

$$\lambda_i(\boldsymbol{x}_0) = \lim_{k\to\infty} \frac{1}{k} \ln |\mu_i(J_k(\boldsymbol{x}_k)\dots J_0(\boldsymbol{x}_0))|, \quad i = 1, \dots, n \qquad (11)$$

where $J_i(\cdot) = \boldsymbol{f}'(\cdot)$ is the Jacobian and $\mu_i(\cdot)$ denote the ith eigenvalue of a matrix (numbered in decreasing order of magnitude). In the continuous-time case, $\dot{\boldsymbol{x}} = \boldsymbol{f}(\boldsymbol{x})$, the leading Lyapunov exponent is defined by

$$\lambda(\boldsymbol{x}_0) = \lim_{t\to\infty} \frac{1}{t} \ln \|\boldsymbol{x}(t;\boldsymbol{x}_0)/\boldsymbol{x}_0\|$$

which is usually evaluated by numerical computations. All Lyapunov exponents depend on the system initial state $\boldsymbol{x}_0$, and reflect the sensitivity with respect to $\boldsymbol{x}_0$.

Lyapunov exponents are generalizations of eigenvalues of linear systems and provide a measure for the mean convergence or divergence rate of neighboring orbits of a dynamical system. For an n-dimensional continuous-time system, depending on the direction (but not the position) of the initial state vector, the n Lyapunov exponents, $\lambda_1 \geq \cdots \geq \lambda_n$, describe different types of attractors. For example, for some nonchaotic attractors (limit sets),

$$\begin{aligned}
&\lambda_i < 0, i = 1, \dots, n \quad \Rightarrow \text{stable equilibrium}\\
&\lambda_1 = 0, \lambda_i < 0, i = 2, \dots, n \quad \Rightarrow \text{stable limit cycle}\\
&\lambda_1 = \lambda_2 = 0, \lambda_i < 0, i = 3, \dots, n \quad \Rightarrow \text{stable two-torus}\\
&\lambda_1 = \cdots = \lambda_m = 0,\\
&\qquad\qquad \lambda_i < 0, i = m+1, \dots, n \quad \Rightarrow \text{stable } m\text{-torus}
\end{aligned}$$

Here, a two-torus is a bagel-shaped surface in three-dimensional space, and an m-torus is its geometrical generalization in $(m + 1)$-dimensional space.

It is now well known that one and two-dimensional continuous-time autonomous dynamical systems cannot produce chaos. For a three-dimensional continuous-time autonomous system, the only possibility for chaos to exist is that the three Lyapunov exponents are

$$(+, 0, -) := (\lambda_1 > 0, \lambda_2 = 0, \lambda_3 < 0) \quad \text{and} \quad \lambda_3 < -\lambda_1$$

Intuitively, this means that the system orbit in the phase space expands in one direction but shrinks in another direction, thereby yielding many complex (stretching and folding) dynamical phenomena within a bounded region. The discrete-time case is different, however. A prominent example is the one-dimensional logistic map, discussed in more detail later, which is chaotic but has (the only) one positive Lyapunov exponent. For four-dimensional continuous-time autonomous systems, there are only three possibilities for chaos to emerge:

1. $(+, 0, -, -)$: $\lambda_1 > 0$, $\lambda_2 = 0$, $\lambda_4 \leq \lambda_3 < 0$; leading to chaos
2. $(+, +, 0, -)$: $\lambda_1 \geq \lambda_2 > 0$, $\lambda_3 = 0$, $\lambda_4 < 0$; leading to "hyperchaos"
3. $(+, 0, 0, -)$: $\lambda_1 > 0$, $\lambda_2 = \lambda_3 = 0$, $\lambda_4 < 0$; leading to a "chaotic two-torus" (this special orbit has not been experimentally observed).

Simple Zero of the Melnikov Function. The Melnikov theory of chaotic dynamics deals with the saddle points of Poincaré maps of continuous solution flows in the phase space. The Melnikov function provides a measure of the distance between the stable and unstable manifolds near a saddle point.

To introduce the Melnikov function, consider a nonlinear oscillator described by the Hamiltonian system

$$\begin{cases} \dot{p} = -\dfrac{\partial H}{\partial q} + \epsilon f_1 \\ \dot{q} = \dfrac{\partial H}{\partial p} + \epsilon f_2 \end{cases}$$

where $\boldsymbol{f} := [f_1(p, q, t), f_2(p, q, t)]^\top$ has state variables $(p(t), q(t))$, $\epsilon > 0$ is small, and $H = H(p, q) = E_K + E_P$ is the Hamilton function for the undamped, unforced (when $\epsilon = 0$) oscillator, in which E_K and E_P are the kinetic and potential energy of the system, respectively. Suppose that the unperturbed (unforced and undamped) oscillator has a saddle-node equilibrium (e.g., the undamped pendulum) and that $\boldsymbol{f}$ is t_p-periodic with phase frequency ω. If the forced motion is described in the three-dimensional phase space (p, q, ωt), then the Melnikov function is defined by

$$F(d^*) = \int_{-\infty}^{\infty} [\nabla H(\overline{p}, \overline{q})] \boldsymbol{f}^* \, dt \tag{12}$$

where ($\overline{p}$, $\overline{q}$) are the solutions of the unperturbed homoclinic orbit starting from the saddle point of the original Hamiltonian system, $\boldsymbol{f}^* = \boldsymbol{f}(\overline{p}, \overline{q}, \omega t + d^*)$, and $\nabla H = [\partial H/\partial p, \partial H/\partial q]$. The variable d^* gives a measure of the distance between the stable and unstable manifolds near the saddle-node equilibrium.

The Melnikov theory states that chaos is possible if the two manifolds interset, which corresponds to the fact that the Melnikov function has a simple zero: $F(d^*) = 0$ at a single point, d^*.

Strange Attractors. Attractors are typical in nonlinear systems. The most interesting attractors, very closely related to chaos, are the strange attractors. A *strange attractor* is a bounded attractor that exhibits sensitive dependence on initial conditions but cannot be decomposed into two invariant subsets contained in disjoint open sets. Most chaotic systems have strange attractors; however, not all strange attractors are associated with chaos.

Generally speaking, a strange attractor is not any of the stable equilibria or limit cycles, but rather consists of some limit sets associated with Cantor sets and/or fractals. In other words, it has a special and complicated structure that may possess a noninteger dimension (fractals) and has some of the properties of a Cantor set. For instance, a chaotic orbit usually appears to be "strange" in that the orbit moves toward a certain point (or limit set) for some time but then moves away from it for some other time. Although the orbit repeats this process infinitely many times it never settles anywhere. Figure 6 shows a typical Chua circuit attractor (2,4,6) that has such strange behavior.

Fractals. An important concept that is related to Lyapunov exponent is the Hausdorff dimension. Let S be a set in R^n and

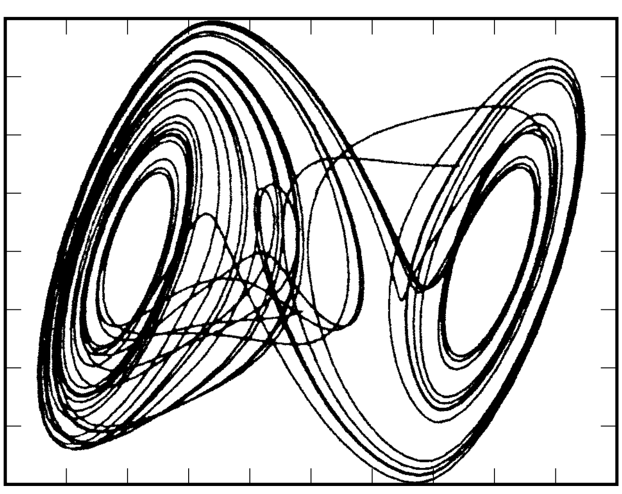

Figure 6. A typical example of stranger attractor: The double scroll of Chua's circuit response.

C be a covering of S by countably many balls of radii d_1, d_2, $\cdots$, satisfying $0 < d_k < \epsilon$ for all k. For a constant $\rho > 0$, consider $\Sigma_{k=1}^{\infty} d_k^{\rho}$ for different coverings, and let $\inf_C \Sigma d_k^{\rho}$ be the smallest value of the sum over all possible such coverings. In the limit $\epsilon \to 0$, this value will diverge if $\rho < h$ but tends to zero if $\rho > h$ for some constant $h \geq 0$ (need not be an integer). This value, h, is called the *Hausdorff dimension* of the set S. If such a limit exists for $\rho = h$, then the *Hausdorff measure* of the set S is defined to be

$$\mu_{\rm h}(S) := \lim_{\epsilon \to 0} \inf_{\rm C} \sum_{k=1}^{\infty} d_k^{\rho}$$

There is an interesting conjecture that the Lyapunov exponents $\{\lambda_k\}$ (indicating the dynamics) and the Hausdorff dimension h (indicating the geometry) of a strange attractor have the relation

$$h = k + \frac{1}{|\lambda_{k+1}|} \sum_{i=1}^{k} \lambda_i, \quad \lambda_1 \geq \lambda_2 \geq \cdots \geq \lambda_n$$

where k is the largest integer that satisfies $\Sigma_{i=1}^{k} \lambda_i > 0$. This formula has been mathematically proved for large families of three-dimensional continuous-time autonomous systems and of two-dimensional discrete-time systems.

A notion that is closely related to the Hausdorff dimension is fractal. Fractal was first coined and defined by Mandelbrot in the 1970s to be a set with Hausdorff dimension strictly greater than its topological dimension (which is always an integer). Roughly, a *fractal* is a set that has a fractional Hausdorff dimension and possesses certain self-similarities. An illustration of the concept of self-similarity and fractal is given in Fig. 13. There is a strong connection between fractal and chaos. Chaotic orbits often possess fractal structures in the phase space. For conservative systems, the Kolmogorov-Arnold-Moser (KAM) theorem implies that the boundary between the region of regular motion and that of chaos is fractal. However, some chaotic systems have nonfractal limit sets, and many fractal structures are not chaotic.

Finite Kolmogorov-Sinai Entropy. Another important feature of chaos and strange attractors is quantified by the Kolmogorov-Sinai (KS) entropy, a concept based on Shannon's information theory.

The familiar statistical entropy is defined by

$$E = -c \sum_k P_k \ln(P_k)$$

where c is a constant and P_k is the probability of the system state being at the stage k of the process. According to Shannon's information theory, this entropy is a measure of the amount of information needed to determine the state of the system. This idea can be used to define a measure for the intensity of a set of system states, which gives the mean loss of information on the state of the system when it evolves with time. To do so, let $\boldsymbol{x}(t)$ be a system orbit and partition its m-dimensional phase space into cells of a small volume, ϵ^m. Let $P_{k_0 \cdots k_i}$ be the joint probability that $\boldsymbol{x}(t = 0)$ is in cell k_0, $\boldsymbol{x}(t = t_s)$ is in cell k_1, . . ., $\boldsymbol{x}(t = it_s)$ is in cell k_i, where $t_s > 0$

is the sampling time. Then Shannon defined the information index to be

$$\mathscr{I}_n := \sum_{k_0,\ldots,k_n} P_{k_0\cdots k_n} \ln\left(P_{k_0\cdots k_n}\right)$$

which is proportional to the amount of the information needed to determine the orbit, if the probabilities are known. Consequently, $\mathscr{I}_{n+1} - \mathscr{I}_n$ gives additional information for predicting the next state if all preceding states are known. This difference is also the information lost during the process. The KS entropy is then defined by

$$\begin{aligned} E_{\mathrm{KS}} &:= \lim_{t_s\to 0}\lim_{\epsilon\to 0}\lim_{n\to\infty} \frac{1}{nt_s}\sum_{i=0}^{n-1}(\mathscr{I}_{i+1} - \mathscr{I}_i) \\ &= -\lim_{t_s\to 0}\lim_{\epsilon\to 0}\lim_{n\to\infty} \frac{1}{nt_s}\sum_{k_0,\ldots,k_{n-1}} P_{k_0\cdots k_{n-1}} \ln\left(P_{k_0\cdots k_{n-1}}\right) \end{aligned} \tag{13}$$

This entropy, E_{KS}, quantifies the degree of disorder: (1) $E_{\mathrm{KS}} = 0$ indicates regular attractors, such as stable equilibria, limit cycles, and tori; (2) $E_{\mathrm{KS}} = \infty$ implies totally random dynamics (which has no correlations in the phase space); and (3) $0 < E_{\mathrm{KS}} < \infty$ signifies strange attractors and chaos.

It is interesting to note that there is a connection between the Lyapunov exponents and the KS entropy:

$$E_{\mathrm{KS}} \le \sum_i \lambda_i^+$$

where $\{\lambda_i^+\}$ are positive Lyapunov exponents of the same system.

Chaos in Control Systems

Chaos is ubiquitous. Chaotic behaviors have been found in many typical mathematical maps such as the logistic map, Arnold's circle map, Hénon map, Lozi map, Ikeda map, Bernoulli shift; in various physical systems, including the Duffing oscillator, van der Pol oscillator, forced pendula, hopping robot, brushless dc motor, rotor with varying mass, Lorenz model, and Rössler system. They are also found in electrical and electronic systems (such as Chua's circuit and electric power systems), digital filters, celestial mechanics (the three-body problem), fluid dynamics, lasers, plasmas, solid states, quantum mechanics, nonlinear optics, chemical reactions, neural networks and fuzzy systems, economic and financial systems, biological systems (heart, brain, and population models), and various Hamiltonian systems (4).

Chaos also exists in many engineering processes and, perhaps unexpectedly, in both continuous-time and discrete-time feedback control systems. For instance, in the continuous-time case, chaos has been found in very simple dynamical systems such as a first-order autonomous feedback system with a time-delay feedback channel, surge tank dynamics under a simple liquid level control system with time-delayed feedback, and several other types of time-delayed feedback control systems. Chaos also exists in automatic gain control loops, which are very popular in industrial applications, such as in many receivers of communication systems. Most fascinating of all, very simple pendula can display complex dynamical phenomena; in particular, pendula subject to linear feedback controls can exhibit even richer bifurcations and chaotic behaviors. For example, a pendulum controlled by a proportional-derivative controller can behave chaotically when the tracking signal is periodic, with energy dissipation, even for the case of small controller gains. In addition, chaos has been found in many engineering applications, such as design of control circuits for switched-mode power conversion equipment, high-performance digital robot controllers, second-order systems containing a relay with hysteresis, and various biochemical control systems.

Chaos also occurs frequently in discrete-time feedback control systems due to sampling, quantization, and roundoff effects. Discrete-time linear control systems with dead-zone nonlinearity have global bifurcations, unstable periodic orbits, scenarios leading to chaotic attractors, and crises of chaotic attractors changing to periodic orbits. Chaos also exists in digitally controlled systems, feedback types of digital filtering systems (either with or without control), and even the linear Kalman filter when numerical truncations are involved.

Many adaptive systems are inherently nonlinear, and thus bifurcation and chaos in such systems are often inevitable. The instances of chaos in adaptive control systems usually come from several possible sources: the nonlinearities of the plant and the estimation scheme, external excitation or disturbances, and the adaptation mechanism. Chaos can occur in typical model-referenced adaptive control (MRAC) and self-tuning adaptive control (STAC) systems, as well as some other classes of adaptive feedback control systems of arbitrary order that contain unmodeled dynamics and disturbances. In such adaptive control systems, typical failure modes include convergence to undesirable local minima and nonlinear self-oscillation, such as bursting, limit cycling, and chaos. In indirect adaptive control of linear discrete-time plants, strange system behaviors can arise due to unmodeled dynamics (or disturbances), bad combination of parameter estimation and control law, and lack of persistency of excitation. For example, chaos can be found in set-point tracking control of a linear discrete-time system of unknown order, where the adaptive control scheme is either to estimate the order of the plant or to track the reference directly.

Chaos also emerges from various types of neural networks. Similar to biological neural networks, most artificial neural networks can display complex dynamics, including bifurcations, strange attractors, and chaos. Even a very simple recurrent two-neuron model with only one self-interaction can produce chaos. A simple three-neuron recurrent neural network can also create period-doubling bifurcations leading to chaos. A four-neuron network and multineuron networks, of course, have higher chances of producing complex dynamical patterns such as bifurcations and chaos. A typical example is cellular neural networks, which have very rich complex dynamical behaviors.

Chaos has also been experienced in some fuzzy control systems. The fact that fuzzy logic can produce complex dynamics is more or less intuitive, inspired by the nonlinear nature of the fuzzy systems. This has been justified not only experimentally but also both mathematically and logically. Chaos has been observed, for example, from a coupled fuzzy control system. The change in the shapes of the fuzzy membership functions can significantly alter the dynamical behavior of a fuzzy control system, potentially leading to the occurrence of chaos.

Many specific examples of chaos in control systems can be given. Therefore, controlling chaos is not only interesting as a subject for scientific research but also relevant to the objectives of traditional control engineering. Simply, it is not an issue that can be treated with ignorance or neglect.

BIFURCATIONS

Associated with chaos is bifurcation, another typical phenomenon of nonlinear dynamical systems that quantifies the change of system properties (such as the number and the stabilities of the system equilibria) due to the variation of system parameters. Chaos and bifurcation have a very strong connection; often they coexist in a complex dynamical system.

Basic Types of Bifurcations

To illustrate various bifurcation phenomena, it is convenient to consider the two-dimensional, parametrized, nonlinear dynamical system

$$\begin{cases} \dot{x} = f(x, y; p) \\ \dot{y} = g(x, y; p) \end{cases} \tag{14}$$

where p is a real and variable system parameter.

Let $(\overline{x}, \overline{y}) = (\overline{x}(t; p_0), \overline{y}(t; p_0))$ be an equilibrium of the system when $p = p_0$, at which $f(\overline{x}, \overline{y}; p_0) = 0$ and $g(\overline{x}, \overline{y}; p_0) = 0$. If the equilibrium is stable (respectively, unstable) for $p > p_0$ but unstable (respectively, stable) for $p < p_0$, then p_0 is a *bifurcation value* of p, and $(0, 0, p_0)$ is a *bifurcation point* in the *parameter space,* (x, y, p). A few examples are given next to distinguish several typical bifurcations.

Transcritical Bifurcation. The one-dimensional system

$$\dot{x} = f(x; p) = px - x^2$$

has two equilibria: $\overline{x}_1 = 0$ and $\overline{x}_2 = p$. If p is varied, then there are two equilibrium curves, as shown in Fig. 7. Since the Jacobian at zero for this one-dimensional system is simply $J = p$, it is clear that for $p < p_0 = 0$, the equilibrium $\overline{x}_1 = 0$ is stable, but for $p > p_0 = 0$ it changes to be unstable. Thus, $(\overline{x}_1, p_0) = (0, 0)$ is a bifurcation point. In the figure, the solid curves indicate stable equilibria and the dashed curves, the unstable ones. $(\overline{x}_2, p_0)$ is another bifurcation point. This type of bifurcation is called the *transcritical bifurcation*.

Saddle-Node Bifurcation. The one-dimensional system

$$\dot{x} = f(x; p) = p - x^2$$

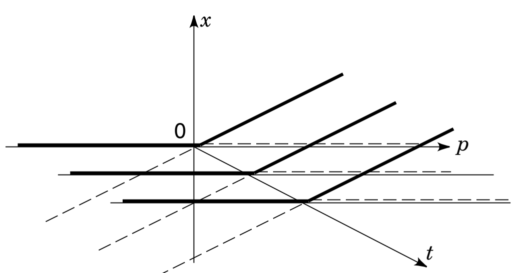

Figure 7. The transcritical bifurcation.

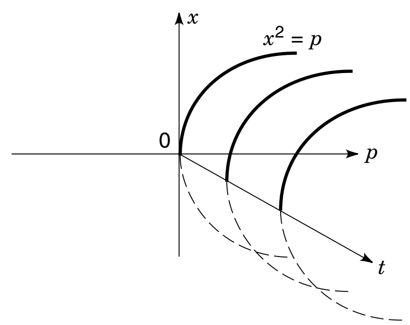

Figure 8. The saddle-node bifurcation.

has an equilibrium $\overline{x}_1 = 0$ at $p_0 = 0$ and an equilibrium curve $\overline{x}_2 = p$ at $p \geq 0$, where $\overline{x}_{21} = \sqrt{p}$ is stable and $\overline{x}_{22} = -\sqrt{p}$ is unstable for $p > p_0 = 0$. This bifurcation, as shown in Fig. 8, is called the *saddle-node bifurcation*.

Pitchfork Bifurcation. The one-dimensional system

$$\dot{x} = f(x; p) = px - x^3$$

has an equilibrium $\overline{x}_1 = 0$ at $p_0 = 0$ and an equilibrium curve $\overline{x}^2 = p$ at $p \geq 0$. Since $\overline{x}_1 = 0$ is unstable for $p > p_0 = 0$ and stable for $p < p_0 = 0$, and since the entire equilibrium curve $\overline{x}^2 = p$ is stable for all $p > 0$ at which it is defined, this situation, as depicted in Fig. 9, is called the *pitchfork bifurcation*.

Note, however, that not all nonlinear parametrized dynamical systems have bifurcations. A simple example is

$$\dot{x} = f(x; p) = p - x^3$$

which has an entire stable equilibrium curve $\overline{x} = p^{1/3}$ and hence does not have any bifurcation.

Hysteresis Bifurcation. The dynamical system

$$\begin{cases} \dot{x}_1 = -x_1 \\ \dot{x}_2 = p + x_2 - x_2^3 \end{cases}$$

has equilibria

$$\overline{x}_1 = 0 \quad \text{and} \quad p - \overline{x}_2 + \overline{x}_2^3 = 0$$

According to different values of p, there are either one or three equilibrium solutions, where the second equation gives

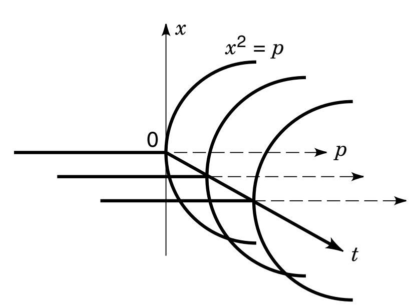

Figure 9. The pitchfork bifurcation.

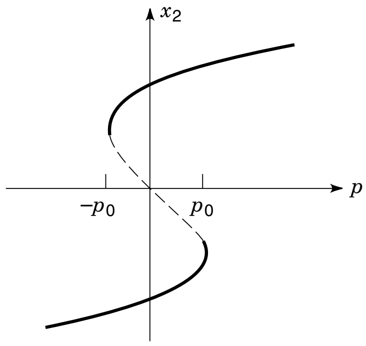

Figure 10. The hysteresis bifurcation.

a bifurcation point at $p_0 = \pm 2\sqrt{3}/9$, but three equilibria for $|p_0| < 2\sqrt{3}/9$.

The stabilities of the equilibrium solutions are shown in Fig. 10. This type of bifurcation is called the *hysteresis bifurcation.*

Hopf Bifurcation and Hopf Theorems. In addition to the bifurcations described previously, called *static bifurcations,* the parametrized dynamical system of Eq. (14) can have another type of bifurcation, the *Hopf bifurcation* (or *dynamical bifurcation*).

Hopf bifurcation corresponds to the situation where, as the parameter p is varied to pass the critical value p_0, the system Jacobian has one pair of complex conjugate eigenvalues moving from the left-half plane to the right, crossing the imaginary axis, while all the other eigenvalues remain to be stable (with negative real parts). At the moment of the crossing, the real parts of the eigenvalue pair are zero, and the stability of the existing equilibrium changes to opposite, as shown in Fig. 11. In the meantime, a limit cycle will emerge. As indicated in the figure, Hopf bifurcation can be classified as *supercritical* (respectively, *subcritical*), if the equilibrium is changed from stable to unstable (respectively, from unstable to stable). The same terminology of supercritical and subcritical bifurcations applies to other non-Hopf types of bifurcations.

Consider the general nonlinear, parametrized autonomous system

$$\dot{\boldsymbol{x}} = \boldsymbol{f}(\boldsymbol{x}; p), \quad \boldsymbol{x}(t_0) = \boldsymbol{x}_0 \tag{15}$$

where $\boldsymbol{x} \in R^n$, p is a real variable parameter, and $\boldsymbol{f}$ is differentiable. The most fundamental result on the Hopf bifurcation of this system is the following theorem, which is stated here for the special two-dimensional case.

Theorem 7 (Poincaré-Andronov-Hopf) Suppose that the two-dimensional system of Eq. (15) has a zero equilibrium, $\overline{\boldsymbol{x}} = 0$, and assume that its associate Jacobian $\boldsymbol{A} = \partial \boldsymbol{f}/\partial \boldsymbol{x}|_{\boldsymbol{x}=\overline{\boldsymbol{x}}=0}$ has a conjugate pair of purely imaginary eigenvalues, $\lambda(p_0)$ and $\lambda^*(p_0)$ for some p_0. Also assume that

$$\left.\frac{d\Re\{\lambda(p)\}}{dp}\right|_{p=p_0} > 0$$

where $\mathscr{R}\{\cdot\}$ denotes the real part of the complex eigenvalues. Then

1. $p = p_0$ is a bifurcation point of the system.
2. For close enough values $p < p_0$, the equilibrium $\overline{\boldsymbol{x}} = 0$ is asymptotically stable.
3. For close enough values $p > p_0$, the equilibrium $\overline{\boldsymbol{x}} = 0$ is unstable.
4. For close enough values $p \neq p_0$, the equilibrium $\overline{\boldsymbol{x}} = 0$ is surrounded by an emerging limit cycle of magnitude $O(\sqrt{|p - p_0|})$.

Graphical Hopf Bifurcation Theorem. The Hopf bifurcation can also be analyzed in the frequency-domain setting (10). In this approach, the nonlinear parametrized autonomous system of Eq. (15) is first rewritten in the following Lur'e form:

$$\begin{cases} \dot{\boldsymbol{x}} = A(p)\boldsymbol{x} + B(p)\boldsymbol{u} \\ \boldsymbol{y} = -C(p)\boldsymbol{x} \\ \boldsymbol{u} = \boldsymbol{g}(\boldsymbol{y}; p) \end{cases} \tag{16}$$

where the matrix $A(p)$ is chosen to be invertible for all values of p, and $\boldsymbol{g} \in C^4$ depends on the chosen matrices A, B, and

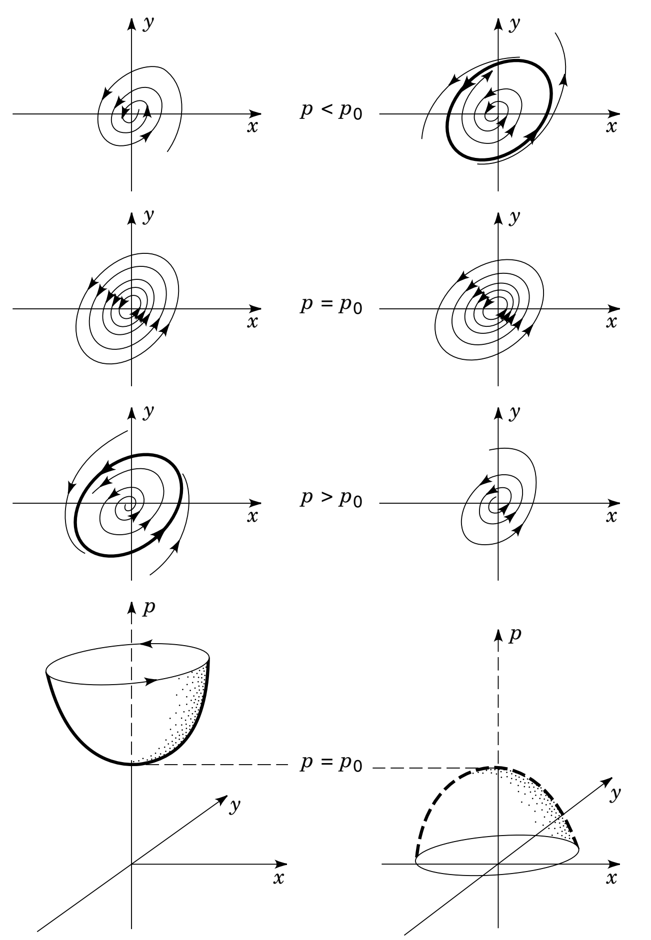

Figure 11. Two types of Hopf bifurcations illustrated in the phase plane. (a) supercritical; (b) subcritical.

C. Assume that this system has an equilibrium solution, $\bar{y}$, satisfying

$$\bar{\boldsymbol{y}}(t;p) = -H(0;p)g(\bar{\boldsymbol{y}}(t;p);p)$$

where

$$H(0;p) = -C(p)A^{-1}(p)B(p)$$

Let $J(p) = \partial \boldsymbol{g}/\partial \boldsymbol{y}|_{y=\bar{y}}$ and let $\hat{\lambda} = \hat{\lambda}(j\omega;\ p)$ be the eigenvalue of the matrix $[H(j\omega;p)J(p)]$ that satisfies

$$\hat{\lambda}(j\omega_0;p_0) = -1 + j0, \quad j = \sqrt{-1}$$

Then fix $p = \tilde{p}$ and let ω vary. In so doing, a trajectory of the function $\hat{\lambda}(\omega;\tilde{p})$, the "eigenlocus," can be obtained. This locus traces out from the frequency $\omega_0 \neq 0$. In much the same way, a real zero eigenvalue (a condition for the *static bifurcation*) is replaced by a characteristic gain locus that crosses the point $(-1 + j\ 0)$ at frequency $\omega_0 = 0$.

For illustration, consider a single-input single-output (SISO) system. In this case, the matrix $[H(j\omega;p)J(p)]$ is merely a scalar, and

$$y(t) \approx \bar{y} + \Re\left\{\sum_{k=0}^{n} y_k e^{jk\omega t}\right\}$$

where $\bar{y}$ is the equilibrium solution and the complex coefficients, $\{y_k\}$, are determined as follows. For the approximation with $n = 2$, first define an auxiliary vector

$$\xi_1(\tilde{\omega}) = \frac{-\boldsymbol{l}^{\mathrm{T}}[H(j\tilde{\omega};\tilde{p})]\boldsymbol{h}_1}{\boldsymbol{l}^{\mathrm{T}}\boldsymbol{r}} \tag{17}$$

where $\tilde{p}$ is the fixed value of the parameter p, $\boldsymbol{l}^{\mathrm{T}}$ and $\boldsymbol{r}$ are the left and right eigenvectors of $[H(j\tilde{\omega};\tilde{p})J(\tilde{p})]$, respectively, associated with the eigenvalue $\hat{\lambda}(j\tilde{\omega};\tilde{p})$, and

$$\boldsymbol{h}_1 = \left[D_2\left(\boldsymbol{z}_{02}\otimes\boldsymbol{r} + \frac{1}{2}\boldsymbol{r}^*\otimes\boldsymbol{z}_{22}\right) + \frac{1}{8}D_3\boldsymbol{r}\otimes\boldsymbol{r}\otimes\boldsymbol{r}^*\right]$$

in which * denotes the complex conjugate, $\tilde{\omega}$ is the frequency of the intersection between the $\hat{\lambda}$ locus and the negative real axis that is closest to the point $(-1 + j\ 0)$, $\otimes$ is the tensor product operator, and

$$D_2 = \left.\frac{\partial^2\boldsymbol{g}(y;\tilde{p})}{\partial y^2}\right|_{y=\bar{y}}$$

$$D_3 = \left.\frac{\partial^3\boldsymbol{g}(y;\tilde{p})}{\partial y^3}\right|_{y=\bar{y}}$$

$$\boldsymbol{z}_{02} = -\frac{1}{4}[1 + H(0;\tilde{p})J(\tilde{p})]^{-1}G(0;\tilde{p})D_2\boldsymbol{r}\otimes\boldsymbol{r}^*$$

$$\boldsymbol{z}_{22} = -\frac{1}{4}[1 + H(2j\tilde{\omega};\tilde{p})]^{-1}H(2j\tilde{\omega};\tilde{p})D_2\boldsymbol{r}\otimes\boldsymbol{r}$$

$$y_0 = \boldsymbol{z}_{02}|\tilde{p} - p_0|$$

$$y_1 = \boldsymbol{r}|\tilde{p} - p_0|^{1/2}$$

$$y_2 = \boldsymbol{z}_{22}|\tilde{p} - p_0|$$

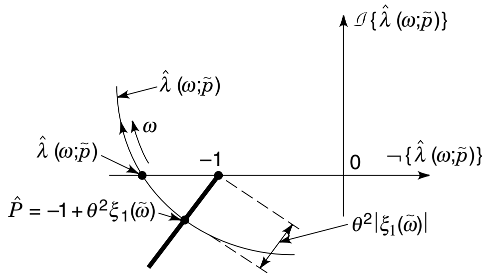

Figure 12. The frequency-domain version of the Hopf bifurcation theorem.

The graphical Hopf bifurcation theorem (for SISO systems) formulated in the frequency domain, based on the generalized Nyquist criterion, is stated as follows (10).

Theorem 8 (Graphical Hopf Bifurcation Theorem) Suppose that when ω varies, the vector $\xi_1(\tilde{\omega}) \neq 0$. Assume also that the half-line, starting from $-1 + j\ 0$ and pointing to the direction parallel to that of $\xi_1(\tilde{\omega})$, first intersects the locus of the eigenvalue $\hat{\lambda}(j\omega;\ \tilde{p})$ at the point

$$\hat{P} = \hat{\lambda}(\hat{\omega};\tilde{p}) = -1 + \xi_1(\tilde{\omega})\theta^2$$

at which $\omega = \hat{\omega}$ and the constant $\theta = \theta(\hat{\omega}) \geq 0$, as shown in Fig. 12. Suppose, furthermore, that the preceding intersection is transversal—namely,

$$\det\begin{bmatrix} \Re\{\xi_1(j\hat{\omega})\} & \mathscr{I}\{\xi_1(j\hat{\omega})\} \\ \Re\left\{\dfrac{d}{d\omega}\hat{\lambda}(\omega;\tilde{p})\Big|_{\omega=\hat{\omega}}\right\} & \mathscr{I}\left\{\dfrac{d}{d\omega}\hat{\lambda}(\omega;\tilde{p})\Big|_{\omega=\hat{\omega}}\right\}\end{bmatrix} \neq 0$$

where $\mathscr{I}\{\cdot\}$ is the imaginary part of the complex eigenvalue. Then

1. The nonlinear system of Eq. (16) has a periodic solution (output) $y(t) = y(t;\ \bar{y})$. Consequently, there exists a unique limit cycle for the nonlinear equation $\dot{\boldsymbol{x}} = \boldsymbol{f}(\boldsymbol{x})$, in a ball of radius $O(1)$ centered at the equilibrium $\bar{\boldsymbol{x}}$.
2. If the total number of counterclockwise encirclements of the point $p_1 = \hat{P} + \epsilon\xi_1(\tilde{\omega})$, for a small enough $\epsilon > 0$, is equal to the number of poles of $[H(s;p)J(p)]$ that have positive real parts, then the limit cycle is stable.

Period-Doubling Bifurcations to Chaos

There are several routes to chaos from a regular state of a nonlinear system, provided that the system is chaotic in nature.

It is known that after three Hopf bifurcations a regular motion can become highly unstable, leading to a strange attractor and, thereafter, chaos. It has also been observed that even pitchfork and saddle-node bifurcations can be routes to chaos under certain circumstances. For motion on a normalized two-torus, if the ratio of the two fundamental frequencies $\omega_1/\omega_2 = p/q$ is rational, then the orbit returns to the same point after a q-cycle; but if the ratio is irrational, the orbit (said to be *quasiperiodic*) never returns to the starting point. Quasiperiodic motion on a two-torus provides another common route to chaos.

Period-doubling bifurcation is perhaps the most typical route that leads system dynamics to chaos. Consider, for example, the logistic map

$$x_{k+1} = px_k(1 - x_k) \tag{18}$$

where $p > 0$ is a variable parameter. With $0 < p < 1$, the origin $x = 0$ is stable, so the orbit approaches it as $k \to \infty$. However, for $1 < p < 3$, all points converge to another equilibrium, denoted $\overline{x}$. The dynamical evolution of the system behavior, as p is gradually increased from 3.0 to 4.0 by small steps, is mostly interesting, which is depicted in Fig. 13. The figure shows that at $p = 3$, a (stable) period-two orbit is bifurcated out of $\overline{x}$, which becomes unstable at that moment, and, in addition to 0, there emerge two (stable) equilibria:

$$\overline{x}_{1,2} = (1 + p \pm \sqrt{p^2 - 2p - 3})/(2p)$$

When p continues to increase to the value of $1 + \sqrt{6} = 3.544090\ldots$, each of these two points bifurcates to the other two, as can be seen from the figure. As p moves consequently through the values $3.568759\ldots$, $3.569891\ldots$, $\cdots$, an infinite sequence of bifurcations is generated by such *period doubling,* which eventually leads to chaos:

$$\text{period } 1 \to \text{period } 2 \to \text{period } 4 \to \cdots \to \text{period } 2^k \to \cdots \to \text{chaos}$$

It is also interesting to note that certain regions (e.g., the three windows magnified in the figure) of the logistic map show self-similarity of the bifurcation diagram of the map, which is a typical fractal structure.

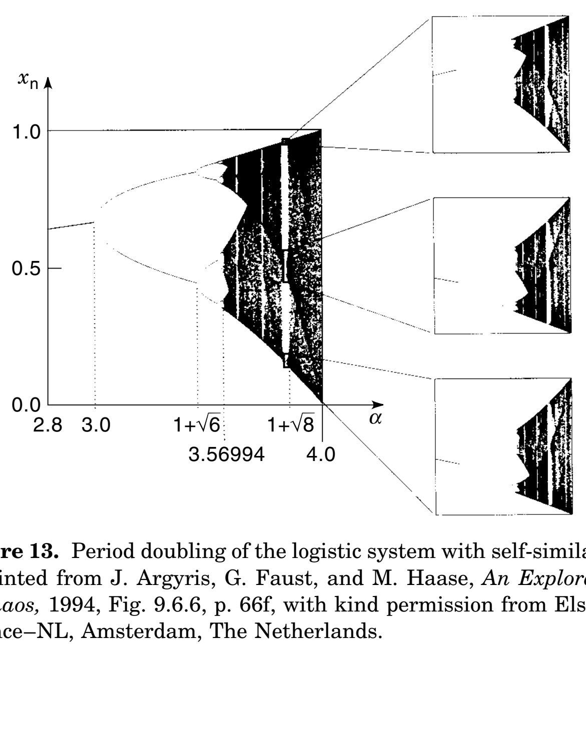

Figure 13. Period doubling of the logistic system with self-similarity. Reprinted from J. Argyris, G. Faust, and M. Haase, *An Exploration of Chaos,* 1994, Fig. 9.6.6, p. 66f, with kind permission from Elsevier Science–NL, Amsterdam, The Netherlands.

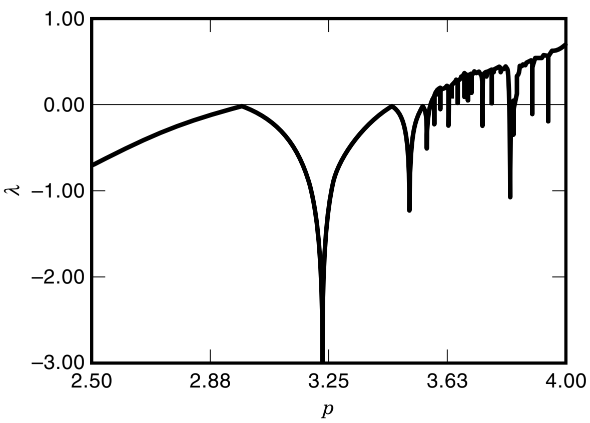

Figure 14. Lyapunov exponent λ versus parameter p for the logistic map. Reprinted from J. Argyris, G. Faust, and M. Haase, *An Exploration of Chaos,* 1994, Fig. 5.4.8.(b), p. 172, with kind permission from Elsevier Science–NL, Amsterdam, The Netherlands.

Figure 14 shows the Lyapunov exponent λ versus the parameter p, in the interval [2.5, 4]. This figure corresponds to the period-doubling diagram shown in Fig. 13.

The most significant discovery about the phenomenon of period-doubling bifurcation route to chaos is Feigenbaum's observation in 1978: The convergence of the period-doubling bifurcating parameters has a geometric rate, $p_\infty - p_k \propto \delta^{-k}$, where

$$\frac{p_{k+1} - p_k}{p_{k+2} - p_{k+1}} \to \delta = 4.6692\ldots \quad (k \to \infty)$$

This is known as a *universal number* for a large class of chaotic dynamical systems.

Bifurcations in Control Systems

Not only chaos but also bifurcations can exist in feedback and adaptive control systems. Generally speaking, local instability and complex dynamical behavior can result from feedback and adaptive mechanisms when adequate process information is not available for feedback transmission or for parameter estimation. In this situation, one or more poles of the linearized closed-loop transfer function may move to cross over the stability boundary, thereby causing signal divergence as the control process continues. However, this sometimes may not lead to global unboundedness, but rather, to self-excited oscillations or self-stabilization, creating very complex dynamical phenomena.

Several examples of bifurcations in feedback control systems include the automatic gain control loop system, which has bifurcations transmitting to Smale horseshoe chaos and the common route of period-doubling bifurcations to chaos. Surprisingly enough, in some situations even a single pendulum controlled by a linear proportional-derivative controller can display rich bifurcations in addition to chaos.

Adaptive control systems are more likely to produce bifurcations than a simple feedback control system due to changes of stabilities in adaptation. The complex dynamics emerging from an adaptive control system are often caused by estimation instabilities. It is known that certain prototypes of MRAC systems can experience various bifurcations.

Bifurcation theory has been employed for analzying complex dynamical systems. For instance, in an MRAC system, a few pathways leading to estimator instability have been identified via bifurcation analysis:

1. A sign change in the adaptation law, leading to a reversal of the gradient direction as well as an infinite linear drift.
2. The instability caused by high control gains, leading to global divergence through period-doubling bifurcations.
3. A Hopf bifurcation type of instability, complicated by a number of nonlocal phenomena, leading to parameter drift and bursting in a bounded regime through a sequence of global bifurcations.

Both instabilities of types 1 and 2 can be avoided by gain tuning or simple algorithmic modifications. The third instability, however, is generally due to the unmodeled dynamics and a poor signal-to-noise ratio, and so cannot be avoided by simple tuning methods. This instability is closely related to the presence of a degenerate set and a period-two attractor.

Similarly, in the discrete-time case, a simple adaptive control system can have rich bifurcation phenomena, such as period-doubling bifurcation (due to high adaptive control gains) and Hopf and global bifurcations (due to insufficient excitation).

Like the omnipresent chaos, bifurcations exist in many physical systems (4). For instance, power systems generally have various bifurcation phenomena. When consumers' demands for power reach peaks, the stability of an electric power network may move to its margin, leading to serious oscillations and stability bifurcations, which may quickly result in voltage collapse. As another example, a typical double pendulum can display bifurcations as well as chaotic motions. Some rotational mechanical systems also have similar behavior. Even a common road vehicle driven by a pilot with driver steering control can have Hopf bifurcation when its stability is lost, which may also develop chaos and even hyperchaos. A hopping robot, or a simple two-degree-of-freedom flexible robot arm, can response strange vibrations undergoing period doubling, which eventually lead to chaos. An aircraft stalling for flight below a critical speed or over a critical angle of attack can cause various bifurcations. Dynamics of a ship can exhibit stability bifurcation according to wave frequencies that are close to the natural frequency of the ship, which creates oscillations and chaotic motions leading the ship to capsize. Simple nonlinear circuits are rich sources of different types of bifurcations as well as chaos. Other systems that have bifurcation properties include cellular neural networks, lasers, aeroengine compressors, weather systems, and biological population dynamics, to name just a few.

CONTROLLING CHAOS

Understanding chaos has long been the main focus of research in the field of nonlinear dynamics. The idea that chaos can be controlled is perhaps counterintuitive. Indeed, the extreme sensitivity of a chaotic system to initial conditions once led to the impression and argument that chaotic motion is in general neither predictable nor controllable.

However, recent research effort has shown that not only (short-term) prediction but also control of chaos are possible. It is now well known that most conventional control methods and many special techniques can be used for controlling chaos (4,11,12). In this pursuit, whether the purpose is to reduce "bad" chaos or to introduce "good" ones, numerous control strategies have been proposed, developed, tested, and applied to many case studies. Numerical and experimental simulations have demonstrated that chaotic physical systems respond quite well to these controls. In about the same time, applications are proposed in such diverse fields as biology, medicine, physiology, chemical engineering, laser physics, electric power systems, fluid mechanics, aerodynamics, circuits and electronic devices, and signal processing and communication. The fact that researchers from vast scientific and engineering backgrounds are joining together and aiming at one central theme—bringing order to chaos—indicates that the study of nonlinear dynamics and their control has progressed into a new era. Much has been accomplished in the past decade, yet much more remains a challenge for the future.

Similar to conventional systems control, the concept of "controlling chaos" first means to suppress chaos in the sense of stabilizing chaotic system responses, often unstable periodic outputs. However, controlling chaos has also encompassed many nontraditional tasks, particularly those of creating or enhancing chaos when it is useful. The process of chaos control is now understood as a transition between chaos and order and, sometimes, the transition from chaos to chaos, depending on the application at hand. In fact, the notion of chaos control is neither exclusive of, nor conflicting with, the purposes of conventional control systems theory. Rather, it targets at better managing the dynamics of a nonlinear system on a wider scale, with the hope that more benefits may be derived from the special features of chaos.

Why Chaos Control?

There are many practical reasons for controlling or ordering chaos. First, "chaotic" (messy, irregular, or disordered) system response with little useful information content is unlikely to be desirable. Second, chaos can lead systems to harmful or even catastrophic situations. In these troublesome cases, chaos should be reduced as much as possible or totally suppressed. Traditional engineering design always tries to reduce irregular behaviors of a system and, therefore, completely eliminates chaos. Such "overdesign" is needed in the aforementioned situations. However, this is usually accomplished at the price of loosing great benefits in achieving high performance near the stability boundaries, or at the expense of radically modifying the original system dynamics.

Ironically, recent research has shown that chaos can actually be useful under certain circumstances, and there is growing interest in utilizing the very nature of chaos (4). For example, it has been observed (13) that a chaotic attractor typically has embedded within it a dense set of unstable limit cycles. Thus, if any of these limit cycles can be stabilized, it may be desirable to select one that characterizes maximal system performance. In other words, when the design of a dynamical system is intended for multiple uses, purposely building chaotic dynamics into the system may allow for the desired flexibilities. A control design of this kind is certainly nonconventional.

Fluid mixing is a good example in which chaos is not only useful but actually necessary (14). Chaos is desirable in many applications of liquid mixing, where two fluids are to be thoroughly mixed while the required energy is minimized. For this purpose, it turns out to be much easier if the dynamics of the particle motion of the two fluids are strongly chaotic, since it is difficult to obtain rigorous mixing properties otherwise due to the possibility of invariant two-tori in the flow. This has been one of the main subjects in fluid mixing, known as "chaotic advection." Chaotic mixing is also important in applications involving heating, such as plasma heating for a nuclear fusion reactor. In such plasma heating, heat waves are injected into the reactor, for which the best result is obtained when the heat convection inside the reactor is chaotic.

Within the context of biological systems, the controlled biological chaos seems to be important with the way a human brain executes its tasks. For years, scientists have been trying to unravel how our brains endow us with inference, thoughts, perception, reasoning, and, most fascinating of all, emotions such as happiness and sadness. It has been suggested that the human brain can process massive information in almost no time, for which chaotic dynamics could be a fundamental reason: "the controlled chaos of the brain is more than an accidental by-product of the brain complexity, including its myriad connections," but rather, "it may be the chief property that makes the brain different from an artificial-intelligence machine" (15). The idea of anticontrol of chaos has been proposed for solving the problem of driving the system responses of a human brain model away from the stable direction and, hence, away from the stable (saddle-type) equilibrium. As a result, the periodic behavior of neuronal population bursting can be prevented (16). Control tasks of this type are also nontraditional.

Other potential applications of chaos control in biological systems have reached out from the brain to elsewhere, particularly to the human heart. In physiology, healthy dynamics has been regarded as regular and predictable, whereas disease, such as fatal arrhythmias, aging, and drug toxicity, is commonly assumed to produce disorder and even chaos. However, recent laboratory studies have seemingly demonstrated that the complex variability of healthy dynamics in a variety of physiological systems has features reminiscent of deterministic chaos, and a wide class of disease processes (including drug toxicities and aging) may actually decrease (yet not completely eliminate) the amount of chaos or complexity in physiological systems (decomplexification). Thus, in contrast to the common belief that healthy heartbeats are completely regular, a normal heart rate may fluctuate in a somewhat erratic fashion, even at rest, and may actually be chaotic (17). It has also been observed that, in the heart, the amount of intracellular Ca^+ is closely regulated by coupled processes that cyclically increase or decrease this amount, in a way similar to a system of coupled oscillators. This cyclical fluctuation in the amount of intracellular Ca^+ is a cause of afterdepolarizations and triggered activities in the heart—the so-called arrhythmogenic mechanism. Medical evidence reveals that controlling (but not completely eliminating) the chaotic arrhythmia can be a new, safe, and promising approach to regulating heartbeats (18,19).

Chaos Control: An Example

To appreciate the challenge of chaos control, consider the one-dimensional logistic map of Eq. (18) with the period-doubling bifurcation route to chaos as shown in Fig. 13. Chaos control problems in this situation include, but are not limited to, the following:

Is it possible (and, if so, how) to design a simple (e.g., linear) controller, u_k, for the given system in the form

$$x_{k+1} = px_k(1 - x_k) + u_k$$

such that

1. The limiting chaotic behavior of the period-doubling bifurcation process is suppressed?
2. The first bifurcation is delayed to take place, or some bifurcations are changed either in form or in stability?
3. When the parameter p is currently not in the bifurcating range, the asymptotic behavior of the system becomes chaotic?

Many of such nonconventional control problems emerging from chaotic dynamical systems have posed a real challenge to both nonlinear dynamics analysts and control engineers—they have become, in effect, motivation and stimuli for the current endeavor devoted to the new research direction in control systems: controlling bifurcations and chaos.

Some Distinctive Features of Chaos Control

At this point, it is illuminating to highlight some distinctive features of chaos control theory and methodology, in contrast to other conventional approaches regarding such issues as objectives, perspectives, problem formulations, and performance measures.

1. The targets in chaos control are usually unstable periodic orbits (including equilibria and limit cycles), perhaps of high periods. The controller is designed to stabilize some of these unstable orbits or to drive the trajectories of the controlled system to switch from one orbit to another. This interorbit switching can be either chaos → order, chaos → chaos, order → chaos, or order → order, depending on the application of interest. Conventional control, on the other hand, does not normally investigate such interorbit switching problems of a dynamical system, especially not those problems that involve guiding the system trajectory to an unstable or chaotic state by any means.
2. A chaotic system typically has embedded within it a dense set of unstable orbits and is extremely sensitive to tiny perturbations in its initial conditions and system parameters. Such a special property, useful for chaos control, is not available in nonchaotic systems and is not utilized in any forms in conventional controls.
3. Most conventional control schemes work within the state space framework. In chaos control, however, one more often deals with the parameter space and phase space. Poincaré maps, delay-coordinates embedding, parametric variation, entropy reduction, and bifurca-

tion monitoring are some typical but nonconventional tools for design and analysis.

4. In conventional control, the terminal time for the control is usually finite (e.g., the elementary concept of "controllability" is typically defined using a finite and fixed terminal time, at least for linear systems and affine-nonlinear systems). However, the terminal time for chaos control is usually infinite to be meaningful and practical, because many nonlinear dynamical behaviors, such as equilibrium states, limit cycles, attractors, and chaos, are asymptotic properties. In addition, in chaos control, a target for tracking is not limited to constant vectors in the state space but often is an unstable periodic orbit of the given system.
5. Depending on different situations or purposes, the performance measure in chaos control can be different from those for conventional controls. Chaos control generally uses criteria like Lyapunov exponents, Kolmogorov-Sinai entropy, power spectra, ergodicity, and bifurcation changes, whereas conventional controls normally emphasize robustness of the system stability or control performance, optimality of control energy or time, ability of disturbances rejection, etc.
6. Chaos control includes a unique task—anticontrol, required by some unusual applications such as those in biomedical engineering mentioned previously. This anticontrol tries to create, maintain, or enhance chaos for improving system performance. Bifurcation control is another example of this kind, where a bifurcation point is expected to be delayed in case it cannot be avoided or stabilized. This delay can significantly extend the operating time (or system parameter range) for a time-critical process such as chemical reaction, voltage collapse of electric power systems, and compression of stall of gas turbine jet engines. These are in direct contrast to traditional control tasks, such as the textbook problem of stabilizing an equilibrium position of a nonlinear system.
7. Due to the inherent association of chaos and bifurcations with various related issues, the scope of chaos control and the variety of problems that chaos control deals with are quite diverse, including creation and manipulation of self-similarity and symmetry, pattern formation, amplitudes of limit cycles and sizes of attractor basins, and birth and change of bifurcations and limit cycles, in addition to some typical conventional tasks, such as target tracking and system regulation.

It is also worth mentioning an additional distinctive feature of a controlled chaotic system that differs from an uncontrolled chaotic system. The controlled chaotic system is generally nonautonomous and cannot be reformulated as an autonomous system by defining the control input as a new state variable, since the controller is physically not a system state variable and, moreover, it has to be determined via design for performance specifications. Hence, a controlled chaotic system is intrinsically much more difficult to design than it appears (e.g., many invariant properties of autonomous systems are no longer valid). This observation raises the question of extending some existing theories and techniques from autonomous system dynamics to nonautonomous, controlled, dynamical systems, including such complex phenomena as degenerate bifurcations and hyperchaos in the system dynamics when a controller is involved. Unless suppressing complex dynamics in a process is the only purpose for control, understanding and utilizing the rich dynamics of a controlled system are very important for design and applications.

Representative Approaches to Chaos Control

There are various conventional and nonconventional control methods available for bifurcations and chaos control (4, 11, 12). To introduce a few representative ones, only three categories of methodologies are briefly described in this section.

Parametric Variation Control. This approach for controlling a chaotic dynamical system, proposed by Ott, Grebogi, and Yorke (13,20) and known as the OGY method, is to stabilize one of its unstable periodic orbits embedded in an existing chaotic attractor, via small time-dependent perturbations of the key system parameter. This methodology utilizes the special feature of chaos that a chaotic attractor typically has embedded within it a dense set of unstable periodic orbits.

To introduce this control strategy, consider a general continuous-time parametrized nonlinear autonomous system

$$\dot{\boldsymbol{x}}(t) = \boldsymbol{f}(\boldsymbol{x}(t), p) \tag{19}$$

where, for illustration, $\boldsymbol{x} = [x\,y\,z]^\top$ denotes the state vector, and p is a system parameter accessible for adjustment. Assume that when $p = p^*$ the system is chaotic, and it is desired to control the system orbit, $\boldsymbol{x}(t)$, to reach a saddle-type unstable equilibrium (or periodic orbit), Γ. Suppose that within a small neighborhood of p^*, that is,

$$p^* - \Delta p_{\max} < p < p^* + \Delta p_{\max} \tag{20}$$

where $\Delta p_{\max} > 0$ is the maximum allowable perturbation, both the chaotic attractor and the target orbit Γ do not disappear (i.e., within this small neighborhood of p^*, there are no bifurcation points of the periodic orbit Γ). Then let P be the underlying Poincaré map and Σ be a surface of cross section of Γ. For simplicity, assume that this two-dimensional hyperplane is orthogonal to the third axis and thus is given by

$$\Sigma = \{[\alpha\beta\gamma]^\top \in R^3 : \gamma = z_0 \text{ (a constant)}\}$$

Moreover, let ξ be the coordinates of the surface of cross section; that is, a vector satisfying

$$\xi_{k+1} = P(\xi_k, p_k)$$

where

$$p_k = p^* + \Delta p_k, \quad |\Delta p_k| \le \Delta p_{\max}$$

At each iteration, $p = p_k$ is chosen to be a constant.

Many distinct unstable periodic orbits within the chaotic attractor can be determined by the Poincaré map. Suppose that an unstable period-one orbit ξ_f^* has been selected, which maximizes certain desired system performance with respect to the dynamical behavior of the system. This target orbit satisfies

$$\xi_f^* = P(\xi_f^*, p^*)$$

The iteration of the map near the desired orbit are then observed, and the local properties of this chosen periodic orbit are obtained. To do so, the map is first locally linearized, yielding a linear approximation of P near ξ_f^* and p^*, as

$$\xi_{k+1} \approx \xi_f^* + L_k(\xi_k - \xi_f^*) + \boldsymbol{v}_k(p_k - p^*) \tag{21}$$

or

$$\Delta\xi_{k+1} \approx L_k \Delta\xi_k + \boldsymbol{v}_k \Delta p_k \tag{22}$$

where

$$\Delta\xi_k = \xi_k - \xi_f^*, \quad \Delta p_k = p_k - p^*,$$
$$L_k = \partial P(\xi_f^*, p^*)/\partial\xi_k, \quad \boldsymbol{v}_k = \partial P(\xi_f^*, p^*)/\partial p_k$$

The stable and unstable eigenvalues, $\lambda_{s,k}$ and $\lambda_{u,k}$ satisfying $|\lambda_{s,k}| < 1 < |\lambda_{u,k}|$, can be calculated from the Jacobian L_k. Let M_s and M_u be the stable and unstable manifolds whose directions are specified by the eigenvectors $\boldsymbol{e}_{s,k}$ and $\boldsymbol{e}_{u,k}$ that are associated with $\lambda_{s,k}$ and $\lambda_{u,k}$, respectively. If $\boldsymbol{g}_{s,k}$ and $\boldsymbol{g}_{u,k}$ are the basis vectors defined by

$$\boldsymbol{g}_{s,k}^{\top}\boldsymbol{e}_{s,k} = \boldsymbol{g}_{u,k}^{\top}\boldsymbol{e}_{u,k} = 1,$$
$$\boldsymbol{g}_{s,k}^{\top}\boldsymbol{e}_{u,k} = \boldsymbol{g}_{u,k}^{\top}\boldsymbol{e}_{s,k} = 0$$

then the Jacobian L_k can be expressed as

$$L_k = \lambda_{u,k}\boldsymbol{e}_{u,k}\boldsymbol{g}_{u,k}^{\top} + \lambda_{s,k}\boldsymbol{e}_{s,k}\boldsymbol{g}_{s,k}^{\top} \tag{23}$$

To start the parametric variation control scheme, one may open a window covering the target equilibrium and wait until the system orbit travels into the window (i.e., until ξ_k falls close enough to ξ_f^*). Then the nominal value of the parameter p_k is adjusted by a small amount Δp_k using a control formula given below in Eq. (24). In so doing, both the location of the orbit and its stable manifold are changed, such that the next iteration, represented by ξ_{k+1} in the surface of cross section, is forced toward the local stable manifold of the original equilibrium. Since the system has been linearized, this control action usually is unable to bring the moving orbit to the target at one iteration. As a result, the controlled orbit will leave the small neighborhood of the equilibrium again and continue to wander chaotically as if there was no control on it at all. However, due to the semi-attractive property of the saddle-nose equilibrium, sooner or later the orbit returns to the window again, but generally is closer to the target due to the control effect. Then the next cycle of iteration starts, with an even smaller control action, to nudge the orbit toward the target.

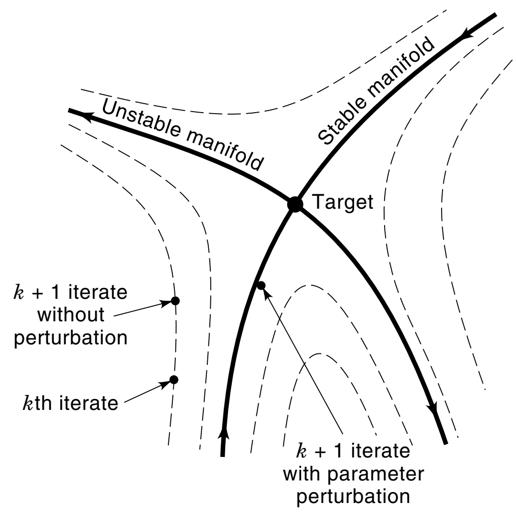

Figure 15. Schematic diagram for the parametric variation control method.

For this case of a saddle-node equilibrium target, this control procedure is illustrated by Fig. 15.

Now suppose that ξ_k has approached sufficiently close to ξ_f^*, so that Eq. (21) holds. For the next iterate, ξ_{k+1}, to fall onto the local stable manifold of ξ_f^*, the parameter $p_k = p^* + \Delta p_k$ has to be so chosen that

$$\boldsymbol{g}_{u,k}^{\top}\Delta\xi_{k+1} = \boldsymbol{g}_{u,k}^{\top}(\xi_{k+1} - \xi_f^*) = 0$$

This simply means that the direction of the next iteration is perpendicular to the direction of the current local unstable manifold. For this purpose, taking the inner product of Eq. (22) with $\boldsymbol{g}_{u,k}$ and using Eq. (23) lead to

$$\Delta p_k = -\lambda_{u,k}\frac{\boldsymbol{g}_{u,k}^{\top}\Delta\xi_k}{\boldsymbol{g}_{u,k}^{\top}\boldsymbol{v}_k} \tag{24}$$

where it is assumed that $\boldsymbol{g}_{u,k}^{\top}\boldsymbol{v}_k \neq 0$. This is the control formula for determining the variation of the adjustable system parameter p at each step, $k = 1, 2, \cdots$. The controlled orbit thus is expected to approach ξ_f^* at a geometric rate.

Note that this calculated Δp_k is used to adjust the parameter p only if $|\Delta p_k| \leq \Delta p_{\max}$. When $|\Delta p_k| > \Delta p_{\max}$, however, one should set $\Delta p_k = 0$. Also, when ξ_{k+1} falls on a local stable manifold of ξ_f^*, one should set $\Delta p_k = 0$ because the stable manifold might lead the orbit directly to the target.

Note also that the preceding derivation is based on the assumption that the Poincaré map, P, always possesses a stable and an unstable direction (saddle-type orbits). This may not be the case in many systems, particularly those with high periodic orbits. Moreover, it is necessary that the number of accessible parameters for control is at least equal to the number of unstable eigenvalues of the periodic orbit to be stabilized. In particular, when some of such key system parameters are unaccessible, the algorithm is not applicable or has to be modified. Also, if a system has multiattractors the system orbit may never return to the opened window but move to another nontarget limit set. In addition, the technique is successful only if the control is applied after the system orbit moves into the small window covering the target, over which the local linear approximation is still valid. In this case, the waiting time can be quite long for some chaotic systems. While this algorithm is effective, it generally requires good knowledge of the equations governing the system, so that computing Δp_k by Eq. (24) is possible. In the case where only time-series data of the system are available, the *delay-coordinate* technique may be used to construct a faithful dynamical model for control (20,21).

Entrainment and Migration Controls. Another representative approach for chaos control is the *entrainment* and *migration* control. Originally an open-loop strategy, this approach has lately been equipped with the closed-loop control technique and has been applied to many complex dynamical systems, particularly those with multiattractors. The entrainment and migration control strategy results in a radical but systematic modification of the behavior of the given dynamical system, thereby allowing to introduce a variety of new dynamical motions into the system (22,23). This approach can handle a multiattractor situation effectively, as opposed to the parametric variation control method.

Entrainment means that an otherwise chaotic orbit of a system can be purposely "entrained" so that its dynamics, in both amplitude and phase, asymptotically tends to a prespecified set or region (e.g., a periodic orbit or an attractor). The basic formulation of entrainment control is based on the existence of some convergent regions in the phase space of a dynamical system. For a general smooth discrete-time system,

$$\boldsymbol{x}_{k+1} = \boldsymbol{f}_k(\boldsymbol{x}_k), \quad k = 0, 1, \ldots$$

or continuous-time system,

$$\dot{\boldsymbol{x}}(t) = \boldsymbol{f}(\boldsymbol{x}(t)), \quad \boldsymbol{x}(0) = \boldsymbol{x}_0$$

the convergent regions are defined to be

$$C(\boldsymbol{f}_k) = \{\boldsymbol{x} \in R^n : \left|\partial f_i(\boldsymbol{x})/\partial x_j - \delta_{ij}\mu_i(\boldsymbol{x})\right| = 0, \\ \left|\mu_i(\boldsymbol{x})\right| < 1 \text{ for all } i = 1, \ldots, n\}$$

or

$$C(\boldsymbol{f}) = \{\boldsymbol{x} \in R^n : \left|\partial f_i(\boldsymbol{x})/\partial x_j - \delta_{ij}\lambda_i(\boldsymbol{x})\right| = 0, \\ \Re\{\lambda_i(\boldsymbol{x})\} < 0 \text{ for all } i = 1, \ldots, n\}$$

where $\mu_i(\cdot)$ and $\lambda_i(\cdot)$ are the eigenvalues of the Jacobians of the nonlinear maps $\boldsymbol{f}_k$ and $\boldsymbol{f}$, respectively, and $\delta_{ij} = 1$ if $i = j$ but $\delta_{ij} = 0$ if $i \neq j$.

If these convergent regions exist, the system orbits—say, $\{\boldsymbol{x}_k\}$ in the discrete case—can be forced by a suitably designed external input to approach (a limit set of) the desired goal dynamics, $\{\boldsymbol{g}_k\}$, in the sense that

$$\lim_{k\to\infty} \|\boldsymbol{x}_k - \boldsymbol{g}_k\| = 0$$

In other words, the system is *entrained* to the goal dynamics.

One advantage of the entrainment control is that the goal dynamics can have any topological characteristics, such as equilibrium, periodic, knotted, and chaotic, provided that the target orbit $\{\boldsymbol{g}_k\}$ is located in some goal region $\{G_k\}$ satisfying $G_k \cap C_k \neq \emptyset$, where C_k $(k = 1, 2, \cdots)$ are convergent regions. For simplicity, assume that $G_k \subset C_k$ with the goal orbit $\boldsymbol{g}_k \in G_k$, $k = 1, 2, \cdots$. Let $C = \cup_{k=1}^{\infty} C_k$, and denote the basin of entrainment for the goal by

$$B = \{\boldsymbol{x}_0 \in R^n : \lim_{k\to\infty} \|\boldsymbol{x}_k - \boldsymbol{g}_k\| = 0\}$$

Once a near entrainment is obtained in the sense that

$$\|\boldsymbol{x}_k - \boldsymbol{g}_k\| \le \epsilon$$

for some small $\epsilon > 0$, another form of control can be applied (i.e., to use migration-goal dynamics between different convergent regions, which allows the system trajectory to travel from one attractor to another). This is the *entrainment-migration* control strategy.

To describe the entrainment-goal control more precisely, consider a discrete-time system of the form

$$\boldsymbol{x}_{k+1} = \boldsymbol{f}_k(\boldsymbol{x}_k), \quad \boldsymbol{x}_k \in R^n$$

Let the goal dynamics be $\{\boldsymbol{g}_k\}$ and S_k be a switching function defined by $S_k = 1$ at some desired steps k but $S_k = 0$ otherwise. The controlled dynamical system is suggested as

$$\boldsymbol{x}_{k+1} = \boldsymbol{f}_k(\boldsymbol{x}_k) + \alpha_k S_k[\boldsymbol{g}_{k+1} - \boldsymbol{f}_k(\boldsymbol{g}_k)]$$

where $0 < \alpha_k \le 1$ are constant control gains determined by the user. The control is initiated, with $S_k = 1$, if the system state has entered the basin B; that is, when the system state enters the basin B at $k = k_b$, the control is turned on for $k \ge k_b$. With $\alpha_k = 1$, it gives

$$\boldsymbol{g}_{k+1} - \boldsymbol{f}_k(\boldsymbol{g}_k) = \boldsymbol{x}_{k+1} - \boldsymbol{f}_k(\boldsymbol{x}_k) = 0, \quad k \ge k_b \tag{25}$$

The desired goal dynamics is then achieved: $\boldsymbol{g}_{k+1} = \boldsymbol{f}(\boldsymbol{g}_k)$ for all $k \ge k_b$. Clearly, in this approach,

$$\boldsymbol{u}_k = \alpha_k S_k[\boldsymbol{g}_{k+1} - \boldsymbol{f}_k(\boldsymbol{g}_k)]$$

is an open-loop controller, which is directly added to the right-hand side of the original system.

A meaningful application of the entrainment control is for multiattractor systems, to which the parametric variation control method is not applicable. Another important application is for a system with an asymptotic goal $\boldsymbol{g}_k \equiv \overline{\boldsymbol{g}}$, an equilibrium of the given system. In this case, the basin of entrainment is a convex region in the phase space:

$$B_e = \{\mathrm{x}_0 \in R^n : \|\boldsymbol{x}_0 - \overline{\boldsymbol{g}}\| < r(\overline{\boldsymbol{g}})\}$$

where

$$r(\overline{\boldsymbol{g}}) = \max_r\{r : \|\boldsymbol{x}_0 - \overline{\boldsymbol{g}}\| < r \Rightarrow \lim_{k\to\infty} \|\boldsymbol{x}_k - \overline{\boldsymbol{g}}\| = 0\}$$

The entrainment-migration control method is straightforward, easily implementable, and flexible in design. However, it requires the dynamics of the system be accurately described by either a map or a differential equation. Also, in order for the system state to be entrained to the given equilibrium, the equilibrium must lie in a particular subset of the convergent region. This can be a technical issue, particularly for higher-dimensional systems. In addition, due to the open-loop nature, process stability is not guaranteed in most cases. The main disadvantage of this approach is that it generally employs sophisticated controllers, which may even be more complicated than the given system.

Engineering Feedback Controls. From a control theoretic point of view, if only suppression of chaos is concerned, chaos control may be considered as a special deterministic nonlinear control problem and so may not be much harder than conventional nonlinear systems control. However, this remains to be a technical challenge to conventional controls when a single controller is needed for stabilizing the chaotic trajectory to multiple targets of different periods.

A distinctive characteristic of control engineering from other disciplines is that it employs some kind of feedback mechanism. In fact, feedback is pervasive in modern control theories and technologies. For instance, the parametric variation control method discussed previously is a special type of feedback control method. In engineering control systems, conventional feedback controllers are used for nonchaotic systems. In particular, linear feedback controllers are often designed for linear systems. It has been widely experienced that with careful design of various conventional controllers, controlling chaotic systems by feedback strategies is not only possible, but indeed quite successful. One basic reason for this success is that chaotic systems, although nonlinear and sensitive to initial conditions with complex dynamical behaviors, belong to deterministic systems by their very nature.

Some Features of Feedback Control. Feedback is one of the most fundamental principles prevalent in the world. The idea of using feedback, originated from Isaac Newton and Gottfried Leibniz some 300 years ago, has been applied in various forms in natural science and modern technology.

One basic feature of conventional feedback control is that, while achieving target tracking, it can guarantee the stability of the overall controlled system, even if the original uncontrolled system is unstable. This implies its intrinsic robustness against external disturbances or internal variations to a certain extent, which is desirable and often necessary for good performance of a required control task. The idea of feedback control always consuming strong control energy perhaps led to a false impression that feedback mechanisms may not be suitable for chaos control due to the extreme sensitive nature of chaos. However, feedback control under certain optimality criteria, such as a minimum control energy constraint, can provide the best performance, including the lowest consumption of control energy. This is not only supported by theory but is also confirmed by simulation with comparison.

Another advantage of using feedback control is that it normally does not change the structure and parameters of the given system, and so whenever the feedback is disconnected the given system retains the original form and properties without modification. In many engineering applications, the system parameters are not feasible or not allowed for direct tuning or replacement. In such cases, state or output feedback control is a practical and desirable strategy.

An additional advantage of feedback control is its automatic fashion in processing control tasks without further human interaction after being designed and implemented. As long as a feedback controller is correctly designed to satisfy the stability criteria and performance specifications, it works on its own. This is important for automation, reducing the dependence on individual operator's skills and avoiding human errors in monitoring the control.

A shortcoming of feedback control methods that employ tracking errors is the explicit or implicit use of reference signals. This has never been a problem in conventional feedback control of nonchaotic systems, where reference signals are always some designated, well-behaved ones. However, in chaos control, quite often a reference signal is an unstable equilibrium or unstable limit cycle, which is difficult (if not impossible) to be physically implemented as a reference input. This critical issue has stimulated some new research efforts (for instance, to use another auxiliary reference as the input in a self-tuning feedback manner).

Engineering feedback control approaches have seen an alluring future in more advanced theories and applications in controlling complex dynamics. Utilization of feedback is among the most inspiring concepts that engineering has ever contributed to modern sciences and advanced technologies.

A Typical Feedback Control Problem. A general feedback approach to controlling a dynamical system, not necessarily chaotic nor even nonlinear, can be illustrated by starting from the following general form of an n-dimensional control system:

$$\dot{\boldsymbol{x}}(t) = \boldsymbol{f}(\boldsymbol{x}, \boldsymbol{u}, t), \quad \boldsymbol{x}(0) = \boldsymbol{x}_0 \tag{26}$$

where, as usual, $\boldsymbol{x}$ is the system state, $\boldsymbol{u}$ is the controller, $\boldsymbol{x}_0$ is a given initial state, and $\boldsymbol{f}$ is a piecewise continuous or smooth nonlinear function satisfying some defining conditions.

Given a reference signal, $\boldsymbol{r}(t)$, which can be either a constant (set-point) or a function (time-varying trajectory), the automatic feedback control problem is to design a controller in, say, the state-feedback form

$$\boldsymbol{u}(t) = \boldsymbol{g}(\boldsymbol{x}, t) \tag{27}$$

where $\boldsymbol{g}$ is generally a piecewise continuous nonlinear function, such that the feedback-controlled system

$$\dot{\boldsymbol{x}}(t) = \boldsymbol{f}(\boldsymbol{x}, \boldsymbol{g}(\boldsymbol{x}, t), t) \tag{28}$$

can achieve the goal of tracking:

$$\lim_{t\to\infty} \|\boldsymbol{x}(t) - \boldsymbol{r}(t)\| = 0 \tag{29}$$

For discrete-time systems, the problem and notation are similar: For a system

$$\boldsymbol{x}_{k+1} = \boldsymbol{f}_k(\boldsymbol{x}_k, \boldsymbol{u}_k) \tag{30}$$

with given target trajectory $\{\boldsymbol{r}_k\}$ and initial state $\boldsymbol{x}_0$, find a (nonlinear) controller

$$\boldsymbol{u}_k = \boldsymbol{g}_k(\boldsymbol{x}_k) \tag{31}$$

to achieve the tracking-control goal:

$$\lim_{k\to\infty} \|\boldsymbol{x}_k - \boldsymbol{r}_k\| = 0 \tag{32}$$

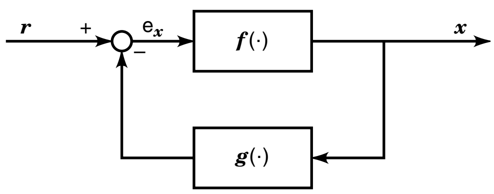

Figure 16. Configuration of a general feedback control system.

A closed-loop continuous-time feedback control system has a configuration as shown in Fig. 16, where $\boldsymbol{e}_x := \boldsymbol{r} - \boldsymbol{g}(\boldsymbol{x})$, $\boldsymbol{f}$ is the given system, and $\boldsymbol{g}$ is the feedback controller to be designed, in which $\boldsymbol{f}$ and $\boldsymbol{g}$ can be either linear or nonlinear. In particular, it can be a linear system in the state-space form connected with a linear additive state-feedback controller—namely,

$$\dot{\boldsymbol{x}} = A\boldsymbol{x} + B\boldsymbol{u} = A\boldsymbol{x} + BK_c(\boldsymbol{r} - \boldsymbol{x})$$

where K_c is a constant control gain matrix to be determined. The corresponding closed-loop block diagram is shown in Fig. 17.

A Control Engineer's Perspective. In controllers design, particularly in finding a nonlinear controller for a system, it is important to emphasize that the designed controller should be (much) simpler than the given system to make sense of the world.

For instance, suppose that one wants to find a nonlinear controller, $u(t)$, in the continuous-time setting, to guide the state vector $\boldsymbol{x}(t) = [x_1(t), \cdots, x_n(t)]^\top$ of a given nonlinear control system,

$$\begin{cases} \dot{x}_1(t) = x_2(t) \\ \dot{x}_2(t) = x_3(t) \\ \quad\vdots \\ \dot{x}_n(t) = f(x_1(t), \ldots, x_n(t)) + u(t) \end{cases}$$

to a target state, $\boldsymbol{y} = [y_1, \ldots, y_n]^\top$—namely,

$$\boldsymbol{x}(t) \to \boldsymbol{y} \quad \text{as} \quad t \to \infty$$

It is then mathematically straightforward to use the controller

$$u(t) = -f(x_1(t), \ldots, x_n(t)) + k_c(x_n(t) - y_n)$$

with an arbitrary constant $k_c < 0$. This controller leads to

$$\dot{x}_n(t) = k_c(x_n(t) - y_n)$$

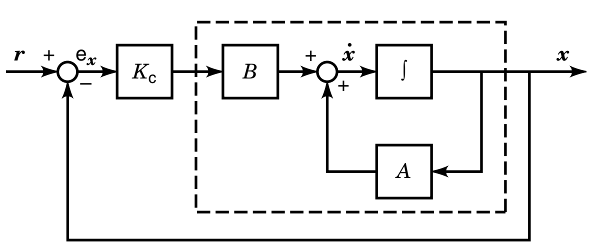

Figure 17. Configuration of a state-space feedback control system.

which yields $e_n(t) := x_n(t) - y_n \to 0$ as $t \to \infty$. Overall, it results in a completely controllable linear system, so that the constant control gain k_c can be chosen such that $\boldsymbol{x}(t) \to \boldsymbol{y}$ as $t \to \infty$. Another example is that for the control system

$$\dot{\boldsymbol{x}}(t) = \boldsymbol{f}(\boldsymbol{x}(t), t) + \boldsymbol{u}(t)$$

using

$$\boldsymbol{u}(t) = -\boldsymbol{f}(\boldsymbol{x}(t), t) + \dot{\boldsymbol{y}}(t) + K(\boldsymbol{x}(t) - \boldsymbol{y}(t))$$

with a stable constant gain matrix K can drive its trajectory to the target $\boldsymbol{y}(t)$ as $t \to \infty$.

This kind of "design," however, is undesirable, and its practical value is questionable in most cases, because the controller is even more complicated than the given system (it cancels the nonlinearity by using the given nonlinearity which means it removes the given plant and then replaces it by another system). In the discrete-time setting, for a given nonlinear system, $\boldsymbol{x}_{k+1} = \boldsymbol{f}_k(\boldsymbol{x}_k) + \boldsymbol{u}_k$, one may also find a similar nonlinear feedback controller or, even simpler, use $\boldsymbol{u} = -\boldsymbol{f}_k(\boldsymbol{x}_k) + \boldsymbol{g}_k(\boldsymbol{x}_k)$ to achieve any desired dynamics satisfying $\boldsymbol{x}_{k+1} = \boldsymbol{g}_k(\boldsymbol{x}_k)$ in just one step. This is certainly not an engineering design, nor a valuable methodology, for any real-world application other than artificial computer simulations.

Therefore, in designing a feedback controller, it is very important to come out with a simplest possible working controller: If a linear controller can be designed to do the job, use a linear controller; otherwise, try the simplest possible nonlinear controllers (starting, for example, from piecewise linear or quadratic controllers). Whether or not one can find a simple, physically meaningful, easily implementable, low-cost, and effective controller for a designated control task can be quite technical: It relies on the designer's theoretical background and practical experience.

A General Approach to Feedback Control of Chaos. To outline the basic idea of a general feedback approach to chaos suppression and tracking control, consider Eq. (26), which is now assumed to be chaotic and possess an unstable periodic orbit (or equilibrium), $\overline{\boldsymbol{x}}$, of period $t_p > 0$—namely, $\overline{\boldsymbol{x}}(t + t_p) = \overline{\boldsymbol{x}}(t)$, $t_0 \le t < \infty$. The task is to design a feedback controller in the form of Eq. (27), such that the tracking control goal of Eq. (29), with $\boldsymbol{r} = \overline{\boldsymbol{x}}$ therein, is achieved.

Since the target periodic orbit $\overline{\boldsymbol{x}}$ is itself a solution of the original system, it satisfies

$$\dot{\overline{\boldsymbol{x}}} = \boldsymbol{f}(\overline{\boldsymbol{x}}, 0, t) \tag{33}$$

Subtracting Eq. (33) from Eq. (26) then yields the error dynamics:

$$\dot{\boldsymbol{e}}_x = \boldsymbol{f}_e(\boldsymbol{e}_x, \overline{\boldsymbol{x}}, t) \tag{34}$$

where

$$\boldsymbol{e}_x(t) = \boldsymbol{x}(t) - \overline{\boldsymbol{x}}(t), \quad \boldsymbol{f}_e(\boldsymbol{e}_x, \overline{\boldsymbol{x}}, t) = \boldsymbol{f}(\boldsymbol{x}, \boldsymbol{g}(\boldsymbol{x}, \overline{\boldsymbol{x}}, t), t) - \boldsymbol{f}(\overline{\boldsymbol{x}}, 0, t)$$

Here, it is important to note that in order to perform correct stability analysis later on, in the error dynamical system of Eq. (34) the function $\boldsymbol{f}_e$ must not explicitly contain $\boldsymbol{x}$; if so, $\boldsymbol{x}$ should be replaced by $\boldsymbol{e}_x + \overline{\boldsymbol{x}}$ (see Eq. (38) below). This is because Eq. (34) should only contain the dynamics of $\boldsymbol{e}_x$ but not

$\boldsymbol{x}$, while the system may contain $\bar{\boldsymbol{x}}$, which merely is a specified time function but not a system variable.

Thus, the design problem becomes to determine the controller, $\boldsymbol{u}(t)$, such that

$$\lim_{t\to\infty} \|\boldsymbol{e_x}(t)\| = 0 \tag{35}$$

which implies that the goal of tracking control described by Eq. (29) is achieved.

It is clear from Eqs. (34) and (35) that if zero is an equilibrium of the error dynamical system of Eq. (34), then the original control problem has been converted to the asymptotic stability problem for this equilibrium. As a result, Lyapunov stability methods and theorems can be directly applied or modified to obtain rigorous mathematical techniques for controller design (24). This is discussed in more detail next.

Chaos Control via Lyapunov Methods. The key in applying the Lyapunov second method to a nonlinear dynamical system is to construct a Lyapunov function that describes some kind of energy and governs the system motion. If this function is constructed appropriately, so that it decays monotonically to zero as time evolves, then the system motion, which falls on the surface of this decaying function, will be asymptotically stabilized to zero. A controller, then, may be designed to force this Lyapunov function of the system, stable or not originally, to decay to zero. As a result, the stability of tracking error equilibrium, and hence the goal of tracking, is achieved. For a chaos control problem with a target trajectory $\bar{\boldsymbol{x}}$, typically an unstable periodic solution of the given system, a design can be carried out by determining the controller $\boldsymbol{u}(t)$ via the Lyapunov second method such that the zero equilibrium of the error dynamics, $\bar{\boldsymbol{e}}_x = 0$, is asymptotically stable.

In this approach, since a linear feedback controller alone is usually not sufficient for the control of a nonlinear system, particularly a chaotic one, it is desirable to find some criteria for the design of simple nonlinear feedback controllers. In so doing, consider the feedback controller candidate of the form

$$\boldsymbol{u}(t) = K_c(\boldsymbol{x} - \bar{\boldsymbol{x}}) + \boldsymbol{g}(\boldsymbol{x} - \bar{\boldsymbol{x}}, \boldsymbol{k}_c, t) \tag{36}$$

where K_c is a constant matrix, which can be zero, and $\boldsymbol{g}$ is a simple nonlinear function with constant parameters $\boldsymbol{k}_c$, satisfying $\boldsymbol{g}(0, \boldsymbol{k}_c, t) = 0$ for all $t \geq t_0$. Both K_c and $\boldsymbol{k}_c$ are determined in the design. Adding this controller to the given system gives

$$\dot{\boldsymbol{x}} = \boldsymbol{f}(\boldsymbol{x}, t) + \boldsymbol{u} = \boldsymbol{f}(\boldsymbol{x}, t) + K_c(\boldsymbol{x} - \bar{\boldsymbol{x}}) + \boldsymbol{g}(\boldsymbol{x} - \bar{\boldsymbol{x}}, \boldsymbol{k}_c, t) \tag{37}$$

The controller is required to drive the trajectory of the controlled system of Eq. (37) to approach the target orbit $\bar{\boldsymbol{x}}$.

The error dynamics of Eq. (34) now takes the form

$$\dot{\boldsymbol{e}}_{\boldsymbol{x}} = \boldsymbol{f}_e(\boldsymbol{e_x}, t) + K_c\boldsymbol{e_x} + \boldsymbol{g}(\boldsymbol{e_x}, \boldsymbol{k}_c, t) \tag{38}$$

where

$$\boldsymbol{e_x} = \boldsymbol{x} - \bar{\boldsymbol{x}}, \quad \boldsymbol{f}_e(\boldsymbol{e_x}, t) = \boldsymbol{f}(\boldsymbol{e_x} + \bar{\boldsymbol{x}}, t) - \boldsymbol{f}(\bar{\boldsymbol{x}}, t)$$

It is clear that $\boldsymbol{f}_e(0, t) = 0$ for all $t \in [t_0, \infty)$—namely, $\bar{\boldsymbol{e}}_x = 0$ is an equilibrium of the tracking-error dynamical system of Eq. (38).

Next, Taylor expand the right-hand side of the controlled system of Eq. (38) at $\boldsymbol{e_x} = 0$ (i.e., at $\boldsymbol{x} = \bar{\boldsymbol{x}}$) and remember that the nonlinear controller will be designed to satisfy $\boldsymbol{g}(0, \boldsymbol{k}_c, t) = 0$. Then the error dynamics is reduced to

$$\dot{\boldsymbol{e}}_{\boldsymbol{x}} = A(\bar{\boldsymbol{x}}, t)\boldsymbol{e_x} + \boldsymbol{h}(\boldsymbol{e_x}, K_c, \boldsymbol{k}_c, t) \tag{39}$$

where

$$A(\bar{\boldsymbol{x}}, t) = \left[\frac{\partial \boldsymbol{f}_e(\boldsymbol{e}_x, t)}{\partial \boldsymbol{e_x}}\right]_{\boldsymbol{e_x}=0}$$

and $\boldsymbol{h}(\boldsymbol{e_x}, K_c, \boldsymbol{k}_c, t)$ contains the rest of the Taylor expansion.

The design is then to determine both the constant control gains K_c and $\boldsymbol{k}_c$ as well as the nonlinear function $\boldsymbol{g}(\cdot, \cdot, t)$ based on the linearized model of Eq. (39), such that $\boldsymbol{e_x} \to 0$ as $t \to \infty$. When this controller is applied to the original system, the goal of both chaos suppression and target tracking will be achieved. For illustration, two controllability conditions established based on the boundedness of the chaotic attractors as well as the Lyapunov first and second methods, respectively, are summarized next (24).

Suppose that in Eq. (39), $\boldsymbol{h}(0, K_c, \boldsymbol{k}_c, t) = 0$ and $A(\bar{\boldsymbol{x}}, t) = A$ is a constant matrix whose eigenvalues all have negative real parts, and let P be the positive definite and symmetric solution of the Lyapunov equation

$$PA + A^{\mathrm{T}}P = -I$$

where I is the identity matrix. If K_c is designed to satisfy

$$\|\boldsymbol{h}(\boldsymbol{e_x}, K_c, \boldsymbol{k}_c, t)\| \leq c\|\boldsymbol{e_x}\|$$

for a constant $c < \frac{1}{2}\lambda_{\max}(P)$ for $t_0 \leq t < \infty$, where $\lambda_{\max}(P)$ is the maximum eigenvalue of P, then the controller $\boldsymbol{u}(t)$, defined in Eq. (36), will drive the trajectory $\boldsymbol{x}$ of the controlled system of Eq. (37) to the target, $\bar{\boldsymbol{x}}$, as $t \to \infty$.

For Eq. (39), since $\bar{\boldsymbol{x}}$ is t_p-periodic, associated with the matrix $A(\bar{\boldsymbol{x}}, t)$ there always exist a t_p-periodic nonsingular matrix $M(\bar{\boldsymbol{x}}, t)$ and a constant matrix Q such that the fundamental matrix (consisting of n independent solution vectors) has the expression

$$\Phi(\bar{\boldsymbol{x}}, t) = M(\bar{\boldsymbol{x}}, t)e^{tQ}$$

The eigenvalues of the constant matrix $e^{t_p Q}$ are called the *Floquet multipliers* of the system matrix $A(\bar{\boldsymbol{x}}, t)$.

In Eq. (39), assume $\boldsymbol{h}(0, K_c, \boldsymbol{k}_c, t) = 0$ and $\boldsymbol{h}(\boldsymbol{e_x}, K_c, \boldsymbol{k}_c, t)$ and $\partial\boldsymbol{h}(\boldsymbol{e_x}, K_c, \boldsymbol{k}_c, t)/\partial\boldsymbol{e_x}$ are both continuous in a bounded neighborhood of the origin in R^n. Assume also that

$$\lim_{\|\boldsymbol{e_x}\|\to 0} \frac{\|\boldsymbol{h}(\boldsymbol{e_x}, K_c, \boldsymbol{k}_c, t)\|}{\|\boldsymbol{e_x}\|} = 0$$

uniformly with respect to $t \in [t_0, \infty)$. If the nonlinear controller of Eq. (36) is so designed that all Floquet multipliers $\{\lambda_i\}$ of the system matrix $A(\bar{\boldsymbol{x}}, t)$ satisfy

$$|\lambda_i(t)| < 1, \quad i = 1, \ldots, n, \quad \forall t \in [t_0, \infty)$$

then the controller will drive the chaotic orbit $\boldsymbol{x}$ of the controlled system of Eq. (37) to the target orbit, $\bar{\boldsymbol{x}}$, as $t \to \infty$.

Various Feedback Methods for Chaos Control. In addition to the general nonlinear feedback control approach described previously, adaptive and intelligent controls are two large classes of engineering feedback control methods that have been shown to be successful for chaos control. Other effective feedback control methods include optimal control, sliding mode and robust controls, digital controls, and occasionally proportional and time-delayed feedback controls. Linear feedback controls are also useful, but generally for simple chaotic systems. Various variants of classical control methods that have demonstrated great potential for controlling chaos include distortion control, dissipative energy method, absorber as a controller, external weak periodic forcing, Kolmogorov-Sinai entropy reduction, stochastic controls, and chaos filtering (4).

Finally, it should be noted that there are indeed many valuable ideas and methodologies that by their nature cannot be well classified into one of the aforementioned three categories, not to mention that many novel approaches are still emerging, improving, and developing as of today (4).

CONTROLLING BIFURCATIONS

Ordering chaos via bifurcation control has never been a subject in conventional control. This seems to be a unique approach valid only for those nonlinear dynamical systems that possess the special characteristic of a route to chaos from bifurcation.

Why Bifurcation Control?

Bifurcation and chaos are often twins and, in particular, period-doubling bifurcation is a route to chaos. Hence, by monitoring and manipulating bifurcations, one can expect to achieve certain types of control for chaotic dynamics.

Even bifurcation control itself is very important. In some physical systems such as a stressed system, delay of bifurcations offers an opportunity to obtain stable operating conditions for the machine beyond the margin of operability in a normal situation. Also, relocating and ensuring stability of bifurcated limit cycles can be applied to some conventional control problems, such as thermal convection, to obtain better results. Other examples include stabilization of some critical situations for tethered satellites, magnetic bearing systems, voltage dynamics of electric power systems, and compressor stall in gas turbine jet engines (4).

Bifurcation control essentially means designing a controller for a system to result in some desired behaviors, such as stabilizing bifurcated dynamics, modifying properties of some bifurcations, or taming chaos via bifurcation control. Typical examples include delaying the onset of an inherent bifurcation, relocating an existing bifurcation, changing the shape or type of a bifurcation, introducing a bifurcation at a desired parameter value, stabilizing (at least locally) a bifurcated periodic orbit, optimizing the performance near a bifurcation point for a system, or a combination of some of these. Such tasks have practical values and great potential in many nontraditional real-world control applications.

Bifurcation Control via Feedback

Bifurcations can be controlled by different methods, among which the feedback strategy is especially effective. Consider a general discrete-time parametrized nonlinear system

$$\boldsymbol{x}_{k+1} = \boldsymbol{f}(\boldsymbol{x}_k; p), \quad k = 0, 1, \ldots \tag{40}$$

where $\boldsymbol{f}$ is assumed to be sufficiently smooth with respect to both the state $\boldsymbol{x}_k \in R^n$ and the parameter $p \in R$, and has an equilibrium at $(\bar{\boldsymbol{x}}, \bar{p}) = (0, 0)$. In addition, assume that the system Jacobian of Eq. (40), evaluated at the equilibrium that is the continuous extension of the origin, has an eigenvalue $\lambda(p)$ satisfying $\lambda(0) = -1$ and $\lambda'(0) \neq 0$, while all remaining eigenvalues have magnitude strictly less than one. Under these conditions, the nonlinear function has a Taylor expansion

$$\boldsymbol{f}(\boldsymbol{x}; p) = J(p)\boldsymbol{x} + Q(\boldsymbol{x}, \boldsymbol{x}; p) + C(\boldsymbol{x}, \boldsymbol{x}, \boldsymbol{x}; p) + \cdots$$

where $J(p)$ is the parametric Jacobian, and Q and C are quadratic and cubic terms generated by symmetric bilinear and trilinear forms, respectively.

This system has the following property (25): A period-doubling orbit can bifurcate from the origin of system of Eq. (40) at $p = 0$; the period-doubling bifurcation is supercritical and stable if $\beta < 0$ but is subcritical and unstable if $\beta > 0$, where

$$\beta = 2\boldsymbol{l}^{\top}[C_0(\boldsymbol{r}, \boldsymbol{r}, \boldsymbol{r}; p) - 2Q_0(\boldsymbol{r}, J_0^{-} Q_0(\boldsymbol{r}, \boldsymbol{r}; p))]$$

in which $\boldsymbol{l}^{\top}$ is the left eigenvector and $\boldsymbol{r}$ the right eigenvector of $J(0)$, respectively, both associated with the eigenvalue -1, and

$$\begin{aligned}
Q_0 &= J(0)Q(\boldsymbol{x}, \boldsymbol{x}; p) + Q(J(0)\boldsymbol{x}, J(0)\boldsymbol{x}; p) \\
C_0 &= J(0)C(\boldsymbol{x}, \boldsymbol{x}, \boldsymbol{x}; p) + 2Q(J(0)\boldsymbol{x}, Q(\boldsymbol{x}, \boldsymbol{x}; p)) \\
&\quad + C(J(0)\boldsymbol{x}, J(0)\boldsymbol{x}, Q(\boldsymbol{x}, \boldsymbol{x}; p); p) \\
J_0^{-} &= [J^{\top}(0)J(0) + \boldsymbol{l}\boldsymbol{l}^{\top}]^{-1} J^{\top}(0)
\end{aligned}$$

Now consider Eq. (40) with a control input:

$$\boldsymbol{x}_{k+1} = \boldsymbol{f}(\boldsymbol{x}_k; p, \boldsymbol{u}_k), \quad k = 0, 1, \ldots$$

which is assumed to satisfy the same assumptions when $\boldsymbol{u}_k = 0$. If the critical eigenvalue -1 is controllable for the linearized system, then there is a feedback controller, $\boldsymbol{u}_k(\boldsymbol{x}_k)$, containing only third-order terms in the components of $\boldsymbol{x}_k$, such that the controlled system has a locally stable bifurcated period-two orbit for p near zero. Also, this feedback stabilizes the origin for $p = 0$. If, however, -1 is uncontrollable for the linearized system, then generically there is a feedback controller, $\boldsymbol{u}_k(\boldsymbol{x}_k)$, containing only second-order terms in the components of $\boldsymbol{x}_k$, such that the controlled system has a locally stable bifurcated period-two orbit for p near 0. This feedback controller also stabilizes the origin for $p = 0$ (25).

Bifurcation Control via Harmonic Balance

For continuous-time systems, limit cycles in general cannot be expressed in analytic forms, and so limit cycles corresponding to the period-two orbits in the period-doubling bifurcation diagram have to be approximated in applications. In this case, the harmonic balance approximation technique (10) can be applied, which is also useful in controlling bifurcations such as delay and stabilization of the onset of period-doubling bifurcations (26).

Consider a feedback control system in the Lur'e form described by

$$\boldsymbol{f} * (\boldsymbol{g} \circ \boldsymbol{y} + K_c \circ \boldsymbol{y}) + \boldsymbol{y} = 0$$

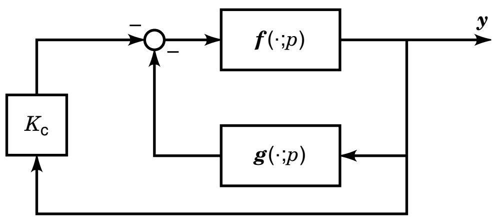

Figure 18. A feedback system in the Lur'e form.

where $*$ and $\circ$ represent the convolution and composition operations, respectively, as shown in Fig. 18. First, suppose that a system $S = S(\boldsymbol{f}, \boldsymbol{g})$ is given as shown in the figure without the feedback controller, K_c. Assume also that two system parameter values, p_h and p_c, are specified, which define a Hopf bifurcation and a supercritical predicted period-doubling bifurcation, respectively. Moreover, assume that the system has a family of predicted first-order limit cycles, stable in the range $p_h < p < p_c$.

Under this system setup, the problem for investigation is to design a feedback controller, K_c, added to the system as shown in Fig. 18, such that the controlled system, $S^* = S^*(\boldsymbol{f}, \boldsymbol{g}, K_c)$, has the following properties:

1. S^* has a Hopf bifurcation at $p_h^* = p_h$.
2. S^* has a supercritical predicted period-doubling bifurcation for $p_c^* > p_c$.
3. S^* has a one-parameter family of stable predicted limit cycles for $p_h^* < p < p_c^*$.
4. S^* has the same set of equilibria as S.

Only the one-dimensional case is discussed here. First, one can design a washout filter with the transfer function $s/(s + a)$, where $a > 0$, such that it preserves the equilibria of the given nonlinear system. Then note that any predicted first-order limit cycle can be well approximated by

$$y^{(1)}(t) = y_0 + y_1 \sin(\omega t)$$

In so doing, the controller transfer function becomes

$$K_c(s) = k_c \frac{s(s^2 + \omega^2(p_h))}{(s+a)^3}$$

where k_c is the constant control gain, and $\omega(p_h)$ is the frequency of the limit cycle emerged from the Hopf bifurcation at the point $p = p_h$. This controller also preserves the Hopf bifurcation at the same point. More importantly, since $a > 0$, the controller is stable, so by continuity in a small neighborhood of k_c the Hopf bifurcation of S^* not only remains supercritical but also has a supercritical predicted period-doubling bifurcation (say at $p_c(k_c)$, close to p_h) and a one-parameter family of stable predicted limit cycles for $p_h < p < p_c(k_c)$.

The design is then to determine k_c such that the predicted period-doubling bifurcation can be delayed, to a desired parameter value p_c^*. For this purpose, the harmonic balance approximation method (10) is useful, which leads to a solution of $y^{(1)}$ by obtaining values of y_0, y_1, and ω (they are functions of p, depending on k_c and a, within the range $p_h < p < p_c^*$). The harmonic balance also yields conditions, in terms of k_c, a and a new parameter, for the period-doubling to occur at the point p_c^*. Thus, the controller design is completed by choosing a suitable value for k_c to satisfy such conditions (26).

Controlling Multiple Limit Cycles

As indicated by the Hopf bifurcation theorem, limit cycles are frequently associated with bifurcations. In fact, one type of *degenerate* (or *singular*) Hopf bifurcations (when some of the conditions stated in the Hopf theorems are not satisfied) determines the birth of multiple limit cycles under system parameters variation. Hence, the appearance of multiple limit cycles can be controlled by manipulating the corresponding degenerate Hopf bifurcations. This task can be conveniently accomplished in the frequency-domain setting.

Again, consider the feedback system of Eq. (16), which can be illustrated by a variant of Fig. 18. For harmonic expansion of the system output, $\boldsymbol{y}(t)$, the first-order formula is (10)

$$\boldsymbol{y}^1 = \theta \boldsymbol{r} + \theta^3 \boldsymbol{z}_{13} + \theta^5 \boldsymbol{z}_{15} + \cdots$$

where θ is shown in Fig. 12, $\boldsymbol{r}$ is defined in Eq. (17), and $\boldsymbol{z}_{13}$, $\cdots$, $\boldsymbol{z}_{1,2m+1}$ are some vectors orthogonal to $\boldsymbol{r}$, $m = 1, 2, \cdots$, given by explicit formulas (10).

Observe that for a given value of $\hat{\omega}$, defined in the graphical Hopf theorem, the SISO system transfer function satisfies

$$H(j\hat{\omega}) = H(s) + (-\alpha + j\delta\omega)H'(s) + \frac{1}{2}(-\alpha + j\delta\omega)^2 H''(s) + \cdots \quad (41)$$

where $\delta\omega = \hat{\omega} - \omega$, with ω being the imaginary part of the bifurcating eigenvalues, and $H'(s)$ and $H''(s)$ are the first and second derivatives of $H(s)$, defined in Eq. (16), respectively. On the other hand, with the higher-order approximations, the following equation of harmonic balance can be derived:

$$[H(j\omega)J + I]\sum_{i=0}^{m} \boldsymbol{z}_{1,2i+1}\theta^{2i+1} = -H(j\omega)\sum_{i=1}^{m} \boldsymbol{r}_{1,2i+1}\theta^{2i+1}$$

where $\boldsymbol{z}_{11} = \boldsymbol{r}$ and $\boldsymbol{r}_{1,2m+1} = \boldsymbol{h}_m$, $m = 1, 2, \cdots$, in which $\boldsymbol{h}_1$ has the formula shown in Eq. (17), and the others also have explicit formulas (10).

In a general situation, the following equation has to be solved:

$$[H(j\hat{\omega})J + I](\boldsymbol{r}\theta + \boldsymbol{z}_{13}\theta^3 + \boldsymbol{z}_{15}\theta^5 + \cdots) = -H(j\hat{\omega})[\boldsymbol{h}_1\theta^3 + \boldsymbol{h}_2\theta^5 + \cdots] \quad (42)$$

In so doing, by substituting Eq. (41) into Eq. (42), one obtains the expansion

$$(\alpha - j\delta\omega) = \gamma_1\theta^2 + \gamma_2\theta^4 + \gamma_3\theta^6 + \gamma_4\theta^8 + O(\theta^9) \quad (43)$$

in which all the coefficients γ_i, $i = 1, 2, 3, 4$, can be calculated explicitly (10). Then taking the real part of Eq. (43) gives

$$\alpha = -\sigma_1\theta^2 - \sigma_2\theta^4 - \sigma_3\theta^6 - \sigma_4\theta^8 - \cdots$$

where $\sigma_i = -\mathscr{R}\{\gamma_i\}$ are the *curvature coefficients* of the expansion.

To this end, notice that multiple limit cycles will emerge when the curvature coefficients are varied near the value zero, after alternating the signs of the curvature coefficients in increasing (or decreasing) order. For example, to have four limit cycles in the vicinity of a type of degenerate Hopf bifurcation that has $\sigma_1 = \sigma_2 = \sigma_3 = 0$ but $\sigma_4 \neq 0$ at the criticality, the system parameters have to be varied in such a way that, for example, $\alpha > 0$, $\sigma_1 < 0$, $\sigma_2 > 0$, $\sigma_3 < 0$, and $\sigma_4 > 0$. This condition provides a methodology for controlling the birth of multiple limit cycles associated with degenerate Hopf bifurcations.

One advantage of this methodology is that there is no need to modify the feedback control path by adding any nonlinear components, to drive the system orbit to a desired region. One can simply modify the system parameters, a kind of parametric variation control, according to the expressions of the curvature coefficients, to achieve the goal of controlling bifurcations and limit cycles.

ANTICONTROL OF CHAOS

Anticontrol of chaos, in contrast to the main stream of ordering or suppressing chaos, is to make a nonchaotic dynamical system chaotic or to retain/enhance the existing chaos of a chaotic system. Anticontrol of chaos as one of the unique features of chaos control has emerged as a theoretically attractive and potentially useful new subject in systems control theory and some time-critical or energy-critical high-performance applications.

Why Anticontrol of Chaos?

Chaos has long been considered as a disaster phenomenon and so is very fearsome in beneficial applications. However, chaos "is dynamics freed from the shackles of order and predictability." Under good conditions or suitable control, it "permits systems to randomly explore their every dynamical possibility. It is exciting variety, richness of choice, a cornucopia of opportunities" (27).

Today, chaos theory has been anticipated to be potentially useful in many novel and time- or energy-critical applications. In addition to those potential utilizations of chaos mentioned earlier in the discussion of chaos control, it is worth mentioning navigation in the multibody planetary system, secure information processing via chaos synchronization, dynamic crisis management, and critical decision making in political, economical, and military events. In particular, it has been observed that a transition of a biological system's state from being chaotic to being pathophysiologically periodic can cause the so-called dynamical disease and so is undesirable. Examples of dynamical diseases include cell counts in hematological disorder; stimulant drug-induced abnormalities in the behavior of brain enzymes and receptors; cardiac interbeat interval patterns in a variety of cardiac disorders; the resting record in a variety of signal sensitive biological systems following desensitization; experimental epilepsy; hormone release patterns correlated with the spontaneous mutation of a neuroendocrine cell to a neoplastic tumor; the prediction of immunologic rejection of heart transplants; the electroencephalographic behavior of the human brain in the presence of neurodegenerative disorder; neuroendocrine, cardiac, and electroencephalographic changes with aging; and imminent ventricular fibrillation in human subjects (28). Hence, preserving chaos in these cases is important and healthy, which presents a real challenge for creative research on anticontrol of chaos (4).

Some Approaches to Anticontrolling Chaos

Anticontrol of chaos is a new research direction. Different methods for anticontrolling chaos are possible (4), but only two preliminary approaches are presented here for illustration.

Preserving Chaos by Small Control Perturbations. Consider an n-dimensional discrete-time nonlinear system

$$\boldsymbol{x}_{k+1} = \boldsymbol{f}(\boldsymbol{x}_k, p, u_k)$$

$\boldsymbol{x}_k$ is the system state, u_k is a scalar-valued control input, p is a variable parameter, and $\boldsymbol{f}$ is a locally invertible nonlinear map. Assume that with $u_k = 0$ the system orbit behaves chaotically at some value of p, and that when p increases and passes a critical value, p_c, inverse bifurcation emerges leading the chaotic state to periodic.

Within the biological context, such a bifurcation is often undesirable: There are many cases where loss of complexity and the emergence of periodicity are associated with pathology (dynamical disease). The question, then, is whether it is possible (if so, how) to keep the system state chaotic even if $p > p_c$, by using small control inputs, $\{u_k\}$.

It is known that there are at least three common bifurcations that can lead chaotic motions directly to low-periodic attracting orbits: (1) crises, (2) saddle-node type of intermittency, and (3) inverse period-doubling type of intermittency. Here, *crisis* refers to sudden changes caused by the collision of an attractor with an unstable periodic orbit; *intermittency* is a special route to chaos where regular orbital behavior is intermittently interrupted by a finite duration "burst" in which the orbit behaves in a decidedly different fashion; and inverse period-doubling bifurcation has a diagram in reverse form to that shown in Fig. 13 (i.e., from chaos back to less and less bifurcating points, leading back to a periodic motion) while the parameter remains increasing.

In all these cases, one can identify a loss region, G, which has the property that after the orbit falls into G, it is rapidly drawn to the periodic orbit. Thus, a strategy to retain the chaos for $p > p_c$ is to avoid this from happening by successively iterating G in such a way that

$$\begin{aligned} G_1 &= \boldsymbol{f}^{-1}(G, p, 0), \\ G_2 &= \boldsymbol{f}^{-1}(G_1, p, 0) = \boldsymbol{f}^{-2}(G, p, 0), \\ &\vdots \\ G_m &= \boldsymbol{f}^{-m}(G, p, 0) \end{aligned}$$

As m increases, the width of G_m in the unstable direction(s) has a general tendency to shrink exponentially. This suggests the following control scheme (28):

> Pick a suitable value of m, denoted m_0. Assume that the orbit initially starts outside the region $G_{m_0+1} \cup G_{m_0} \cup \cdots \cup G_1 \cup G$. If the orbit lands in G_{m_0+1} at iterate ℓ, the control u_ℓ is applied to kick the orbit out of G_{m_0} at the next iterate. Since G_{m_0} is thin, this

control can be very small. After the orbit is kicked out of G_{m_0}, it is expected to behave chaotically, until it falls again into G_{m_0+1}; at that moment another small control is applied, and so on. This procedure can keep the motion chaotic.

Anticontrol of Chaos via State Feedback. An approach to anticontrol of discrete-time systems can be made mathematically rigorous by applying the engineering feedback control strategy. This anticontrol technique is first to make the Lyapunov exponents of the controlled system either strictly positive or arbitrarily assigned (positive, zero, and negative in any desired order), and then apply the simple mod operations (4,29). This task can be accomplished for any given higher-dimensional discrete-time dynamical system that could be originally nonchaotic or even asymptotically stable. The argument used is purely algebraic and the design procedure is completely schematic without approximations.

Specifically, consider a nonlinear dynamical system, not necessarily chaotic nor unstable to start with, in the general form

$$\boldsymbol{x}_{k+1} = \boldsymbol{f}_k(\boldsymbol{x}_k) \tag{44}$$

where $\boldsymbol{x}_k \in R^n$, $\boldsymbol{x}_0$ is given, and $\boldsymbol{f}_k$ is assumed to be continuously differentiable, at least locally in the region of interest.

The anticontrol problem for this dynamical system is to design a linear state-feedback control sequence, $\boldsymbol{u}_k = B_k\boldsymbol{x}_k$, with uniformly bounded constant control gain matrices, $\|B_k\|_s \leq \gamma_{\boldsymbol{u}} < \infty$, where $\|\cdot\|_s$ is the spectral norm for a matrix, such that the output states of the controlled system

$$\boldsymbol{x}_{k+1} = \boldsymbol{f}_k(\boldsymbol{x}_k) + \boldsymbol{u}_k$$

behaves chaotically within a bounded region. Here, chaotic behavior is in the mathematical sense of Devaney described previously—namely, the controlled map (a) is transitive, (b) has sensitive dependence on initial conditions, and (c) has a dense set of periodic solutions (9).

In the controlled system

$$\boldsymbol{x}_{x+1} = \boldsymbol{f}_k(\boldsymbol{x}_k) + B_k\boldsymbol{x}_k$$

let

$$J_k(\boldsymbol{x}_k) = \boldsymbol{f}'_k(\boldsymbol{x}_k) + B_k$$

be the system Jacobian, and let

$$T_k(\boldsymbol{x}_0) = J_k(\boldsymbol{x}_k)\cdots J_1(\boldsymbol{x}_1)J_0(\boldsymbol{x}_0),\ k = 0, 1, 2, \ldots$$

Moreover, let $\mu_i^k = \mu_i(T_k^\top T_k)$ be the ith eigenvalue of the kth product matrix $[T_k^\top T_k]$, where $i = 1, \cdots, n$ and $k = 0, 1, 2, \cdots$.

The first attempt is to determine the constant control gain matrices, $\{B_k\}$, such that the Lyapunov exponents of the controlled system are all finite and strictly positive:

$$0 < c \leq \lambda_i(\boldsymbol{x}_0) < \infty, \quad i = 1, \ldots, n \tag{45}$$

It turns out that this is possible under a natural condition that all the Jacobians $\{\boldsymbol{f}'_k(\boldsymbol{x}_k)\}$ are uniformly bounded:

$$\sup_{0\leq k\leq\infty} \|\boldsymbol{f}'_k(\boldsymbol{x}_k)\| \leq \gamma_{\boldsymbol{f}} < \infty \tag{46}$$

To come up with a design methodology, first observe that if $\{\theta_i^{(k)}\}_{i=1}^n$ are the singular values of the matrix $T_k(\boldsymbol{x}_0)$; then $\theta_i^{(k)} \geq 0$ for all $i = 1, \cdots, n$ and $k = 0, 1, \cdots$. Let $\sigma_i = 0$ for $\theta_i^{(k)} = 0$ and

$$\sigma_i = \lim_{k\to\infty} \frac{1}{k} \ln \theta_i^{(k)} \quad (\text{for } \theta_i^{(k)} > 0), \quad i = 1, \ldots, n$$

Clearly, if $\theta_i^{(k)} = e^{(k+1)\sigma_i}$ is used in the design, then all $\theta_i^{(k)}$ will not be zero for any finite values of σ_i, for all $i = 1, \cdots, n$ and $k = 0, 1, \cdots$. Thus, $T_k(\boldsymbol{x}_0)$ is always nonsingular. Consequently, a control-gain sequence $\{B_k\}$ can be designed such that the singular values of the matrix $T_k(\boldsymbol{x}_0)$ are exactly equal to $\{e^{k\sigma_i}\}_{i=1}^n$: At the kth step, $k = 0, 1, 2, \cdots$, one may simply choose the control gain matrix to be

$$B_k = (\gamma_{\boldsymbol{f}} + e^c)I_n, \quad \text{for all } k = 0, 1, 2, \ldots$$

where the constants c and γ_f are given in Eqs. (45) and (46), respectively (29). This ensures Eq. (45) to hold.

Finally, in conjunction with the previously designed controller—that is,

$$\boldsymbol{u}_k = B_k\boldsymbol{x}_k = (\gamma_{\boldsymbol{f}} + e^c)\boldsymbol{x}_k$$

anticontrol can be accomplished by imposing the mod operation in the controlled system:

$$\boldsymbol{x}_{k+1} = \boldsymbol{f}_k(\boldsymbol{x}_k) + \boldsymbol{u}_k \pmod 1$$

This results in the expected chaotic system whose trajectories remain within a bounded region in the phase space and, moreover, satisfies the aforementioned three basic properties that together define discrete chaos. This approach yields rigorous anticontrol of chaos for any given discrete-time systems, including all higher-dimensional, linear time-invariant systems; that is, with $\boldsymbol{f}_k(\boldsymbol{x}_k) = A\boldsymbol{x}_k$ in Eq. (44), where the constant matrix A can be arbitrary (even asymptotically stable).

Although $\boldsymbol{u}_k = B_k\boldsymbol{x}_k$ is a linear state-feedback controller, it uses full-order state variables, and the mod operation is inherently nonlinear. Hence, other types of (simple) feedback controllers are expected to be developed in the near future for rigorous anticontrol of chaos, particularly for continuous-time dynamical systems [which is apparently much more difficult (30), especially if small control input is desired].

BIBLIOGRAPHY

1. *The New Encyclopaedia Britannica* (Ready Reference and Index), Micropaedia, Vol. 2, Chicago: Encyclopaedia Britannica, Inc., 1984, p. 743.
2. T. Matsumoto, Chaos in electronic circuits, *Proceedings of the IEEE,* **75**: 1033–1057, 1987.

3. *Academic American Encyclopaedia,* Vol. 4, Danbury, CT: Grolier, 1986, p. 283.
4. G. Chen and X. Dong, *From Chaos to Order: Methodologies, Perspectives, and Applications,* Singapore: World Scientific, 1998.
5. G. Chen and J. L. Moiola, An overview of bifurcation, chaos and nonlinear dynamics in control systems, *J. Franklin Inst.,* **331B**: 819–858, 1994.
6. G. Chen, Representation, approximation, and identification, in W. K. Chen (ed.), *The Circuits and Filters Handbook,* Boca Raton, FL: CRC Press, 1995, pp. 973–1006.
7. S. Wiggins, *Introduction to Applied Nonlinear Dynamical Systems and Chaos,* New York: Springer-Verlag, 1990.
8. T. Y. Li and J. A. Yorke, Period three implies chaos, *Amer. Math. Monthly,* **82**: 481–485, 1975.
9. R. L. Devaney, *An Introduction to Chaotic Dynamical Systems,* Reading, MA: Addison-Wesley, 1987.
10. J. L. Moiola and G. Chen, *Hopf Bifurcation Analysis: A Frequency Domain Approach,* Singapore: World Scientific Pub., 1996.
11. G. Chen and X. Dong, From chaos to order—perspectives and methodologies in controlling chaotic nonlinear dynamical systems, *Int. J. Bifur. Chaos,* **3**: 1363–1409, 1993.
12. M. J. Ogorzalek, Taming chaos—part II: Control. *IEEE Trans. Circuits Syst. I, Fundam. Theory Appl.,* **40**: 700–706, 1993.
13. E. Ott, C. Grebogi, and J. A. Yorke, Controlling chaos, *Phys. Rev. Lett.,* **64**: 1196–1199, 1990.
14. J. M. Ottino, *The Kinematics of Mixing: Stretching, Chaos, and Transport,* New York: Cambridge Univ. Press, 1989.
15. W. J. Freeman, The physiology of perception, *Sci. Amer.,* 78–85, Feb. 1991.
16. S. J. Schiff et al., Controlling chaos in the brain, *Nature,* **370**: 615–620, 1994.
17. A. L. Goldberger, Applications of chaos to physiology and medicine, in J. Kim and J. Stringer (eds.), *Applied Chaos,* New York: Academic Press, 1992, pp. 321–331.
18. A. Garfinkel et al., Controlling cardiac chaos, *Science,* **257**: 1230–1235, 1992.
19. J. N. Weiss et al., Chaos and chaos control in biology, *J. Clinical Invest.,* **93**: 1355–1360, 1994.
20. T. Shinbrot et al., Using small perturbations to control chaos, *Nature,* **363**: 411–417, 1993.
21. D. Auerbach et al., Controlling chaos in high dimensional systems, *Phys. Rev. Lett.,* **69**: 3479–3482, 1992.
22. E. A. Jackson, On the control of complex dynamic systems, *Physica D,* **50**: 341–366, 1991.
23. E. A. Jackson, OPCL migration controls between five attractors of the Chua system, *Int. J. Bifur. Chaos,* **5**: 1255–1260, 1995.
24. G. Chen, On some controllability conditions for chaotic dynamics control, *Chaos, Solitions & Fractals,* **8**: 1461–1470, 1997.
25. E. H. Abed, H. O. Wang, and R. C. Chen, Stabilization of period doubling bifurcations and implications for control of chaos. *Physica D,* **70**: 154–164, 1994.
26. A. Tesi et al., Harmonic balance analysis of period-doubling bifurcations with implications for control of nonlinear dynamics, *Automatica,* **32**: 1255–1271, 1996.
27. J. Ford, What is chaos, that we should be mindful of it?, in P. Davies (ed.), *The New Physics,* New York: Cambridge Univ. Press, 1989, pp. 348–372.
28. W. Yang et al., Preserving chaos: Control strategies to preserve complex dynamics with potential relevance to biological disorders. *Phys. Rev. E.,* **51**: 102–110, 1995.
29. G. Chen and D. Lai, Feedback control of Lyapunov exponents for discrete-time dynamical systems, *Int. J. Bifur., Chaos,* **6**: 1341–1349, 1996.
30. T. S. Parker and L. O. Chua, *Practical Numerical Algorithms for Chaotic Systems,* New York: Springer-Verlag, 1989.

GUANRONG CHEN
University of Houston